Geological Survey of Canada

CURRENT RESEARCH
2003-C21

Gold mineralization within the Red Lake mine trend: example from the Cochenour-Willans mine area, Red Lake, Ontario, with new key information from the Red Lake mine and potential analogy with the Timmins camp

Benoît Dubé, Kenneth Williamson, and M. Malo

2003

CURRENT RESEARCH

Natural Resources Canada | Ressources naturelles Canada

Canada

106-03546/

©Her Majesty the Queen in Right of Canada 2003
ISSN 1701-4387

Available in Canada from the
Geological Survey of Canada Bookstore website at:
http://www.nrcan.gc.ca/gsc/bookstore (Toll-free: 1-888-252-4301)

A copy of this publication is also available for reference by depository libraries across Canada through access to the Depository Services Program's website at http://dsp-psd.pwgsc.gc.ca

All requests for permission to reproduce this work, in whole or in part, for purposes of commercial use, resale, or redistribution shall be addressed to: Earth Sciences Sector Information Division, Room 402, 601 Booth Street, Ottawa, Ontario K1A 0E8.

Authors' addresses

Benoît Dubé *(bdube@nrcan.gc.ca)*
Commission géologique du Canada
880, chemin Sainte-Foy
Québec (Quebec) G1S 2L2

Kenneth Williamson *(kwilliam@nrcan.gc.ca)*
Michel Malo *(ess-inrs-nmalo@x1.nrcan.gc.ca)*
INRS Eau, Terre et Environnement
880, chemin Sainte-Foy
Québec (Quebec) G1S 2L2

Publication approved by GSC Quebec

Gold mineralization within the Red Lake mine trend: example from the Cochenour-Willans mine area, Red Lake, Ontario, with new key information from the Red Lake mine and potential analogy with the Timmins camp

Benoît Dubé, Kenneth Williamson, and M. Malo

Dubé, B., Williamson, K., and Malo, M., 2003: Gold mineralization within the Red Lake mine trend: example from the Cochenour-Willans mine area, Red Lake, Ontario, with new key information from the Red Lake mine and potential analogy with the Timmins camp; Geological Survey of Canada, Current Research 2003-C21, 15 p.

Abstract: Detailed mapping of a large stripped outcrop revealed low-grade colloform-crustiform cockade ankerite veins and breccia and ankerite-quartz veins hosted by mafic-ultramafic Balmer assemblage volcanic rocks. Most ankerite veins and breccia are at high angle to and/or crenulated by S_2, suggesting that they are pre- to early-D_2 deformation. Gold mineralization is associated with arsenopyrite hosted by brecciated, more or less silicified ankerite veins and breccia and a high-grade silicified zone. Numerous east-trending 'black line faults' cut all rock types. The Cochenour and Red Lake mines are on the limbs of a F_1 fold refolded by F_2 folds with associated east-southeast syn-D_2 deformation zones. Local andalusite-rich and carbonate-vein clasts in the Huston conglomerate underground at the Red Lake mine indicate protracted or multistage alteration events with pre- and early-D_2 carbonatization and aluminous alteration and some late carbonatization. A regional unconformity (Huston conglomerate) represents a key empirical exploration target because 94% of the 27.6 M oz Au found in the district is in three deposits adjacent to the unconformity.

Résumé : La cartographie détaillée d'un grand affleurement décapé a dévoilé des brèches et veines d'ankérite à texture colloforme-crustiforme ou en cocarde et des veines d'ankérite-quartz faiblement minéralisées dans les roches volcaniques mafiques-ultramafiques de l'assemblage de Balmer. La plupart de ces brèches et veines d'ankérite forment un angle important avec S_2 ou présentent une crénulation par S_2, ce qui laisse croire qu'elles sont antérieures à la déformation D_2, ou contemporaines du début de celle-ci. La minéralisation d'or est associée à l'arsénopyrite dans des brèches et veines d'ankérite bréchifiées et plus ou moins silicifiées, ainsi que dans une zone silicifiée à forte teneur. De nombreuses « failles à trait noir » de direction est recoupent tous les types de roches. Les mines Cochenour et Red Lake se trouvent sur les flancs d'un pli P_1 repris par des plis P_2, auxquels sont associés des zones de déformation de direction est–sud-est contemporaines de la déformation D_2. Sous terre à la mine Red Lake, la présence, par endroits, de clastes riches en andalousite et de clastes de veines de carbonates dans le conglomérat de Huston témoigne d'une altération prolongée ou en plusieurs étapes. Une carbonatisation et une altération alumineuse ont précédé et accompagné les phase précoces de D_2 et une certaine carbonatisation s'est déroulée plus tard. Une discordance régionale (conglomérat de Huston) constitue une cible empirique d'exploration de première importance puisque 94 % des 27,6 millions d'onces d'or trouvés dans le district sont contenus dans trois gisements qui lui sont adjacents.

INTRODUCTION

The Cochenour-Willans mine, the fourth largest gold mine in the Red Lake district, has produced a total of 36.31 t of gold from 1 931 730 tonnes at an average grade of 18.8 g/t between 1939 and 1971 (Giancola, 1999). Resources are estimated at 157 000 t grading 17.5 g/t Au (Giancola, 1994). The Cochenour-Willans mine area in the northwestern portion of the Red Lake mine trend provides an opportunity to study key geological parameters controlling gold mineralization within the trend and to assist in developing exploration guidelines for here and elsewhere (Fig. 1).

In the summer of 2002, detailed mapping was done over one large stripped outcrop near the No. 1 shaft of the former Cochenour-Willans mine, a few surface exposures and stripped outcrops within the Red Lake mine trend, and underground at the Red Lake mine. As the Cochenour-Willans mine has been closed for many years, the large stripped outcrop mapped provided an opportunity to study geological parameters and key chronological relationships between hydrothermal alteration, mineralization, deformation, and metamorphism in the area. The goal of this report is to describe the geology of gold mineralization in the Cochenour-Willans mine area and to discuss its significance at the scale of the Red Lake mine trend, as part of our ongoing study of gold mineralization in the Red Lake district (Dubé et al., 2000, 2001a, b, 2002; Chi et al., 2002). New information from the Red Lake mine is also provided. A 1:150 map is planned for release as a GSC Open File (B. Dubé and K. Williamson, work in progress, 2003) and will complement this report.

REGIONAL GEOLOGICAL SETTING

The Red Lake regional geological setting is summarized in Sanborn-Barrie et al. (2000, 2001) and Dubé et al. (2001a). A regional perspective and synthesis of alteration and gold mineralization in the district is given in Parker (2002).

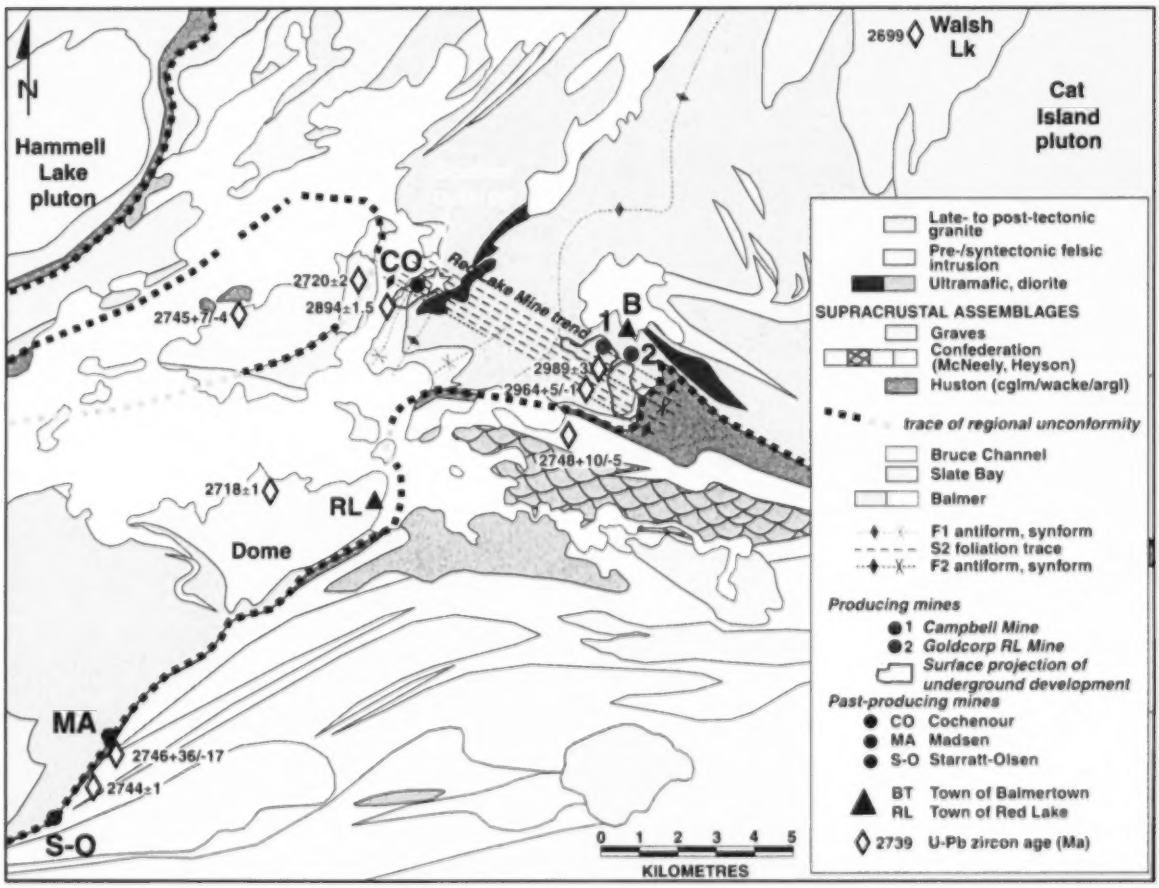

Figure 1. *Geology of Red Lake mine trend area (*modified from *Sanborn-Barrie et al., 2001, and Goldcorp geological data).*

INTRODUCTION

The Cochenour-Willans mine, the fourth largest gold mine in the Red Lake district, has produced a total of 36.31 t of gold from 1 931 730 tonnes at an average grade of 18.8 g/t between 1939 and 1971 (Giancola, 1999). Resources are estimated at 157 000 t grading 17.5 g/t Au (Giancola, 1994). The Cochenour-Willans mine area in the northwestern portion of the Red Lake mine trend provides an opportunity to study key geological parameters controlling gold mineralization within the trend and to assist in developing exploration guidelines for here and elsewhere (Fig. 1).

In the summer of 2002, detailed mapping was done over one large stripped outcrop near the No. 1 shaft of the former Cochenour-Willans mine, a few surface exposures and stripped outcrops within the Red Lake mine trend, and underground at the Red Lake mine. As the Cochenour-Willans mine has been closed for many years, the large stripped outcrop mapped provided an opportunity to study geological parameters and key chronological relationships between hydrothermal alteration, mineralization, deformation, and metamorphism in the area. The goal of this report is to describe the geology of gold mineralization in the Cochenour-Willans mine area and to discuss its significance at the scale of the Red Lake mine trend, as part of our ongoing study of gold mineralization in the Red Lake district (Dubé et al., 2000, 2001a, b, 2002; Chi et al., 2002). New information from the Red Lake mine is also provided. A 1:150 map is planned for release as a GSC Open File (B. Dubé and K. Williamson, work in progress, 2003) and will complement this report.

REGIONAL GEOLOGICAL SETTING

The Red Lake regional geological setting is summarized in Sanborn-Barrie et al. (2000, 2001) and Dubé et al. (2001a). A regional perspective and synthesis of alteration and gold mineralization in the district is given in Parker (2002).

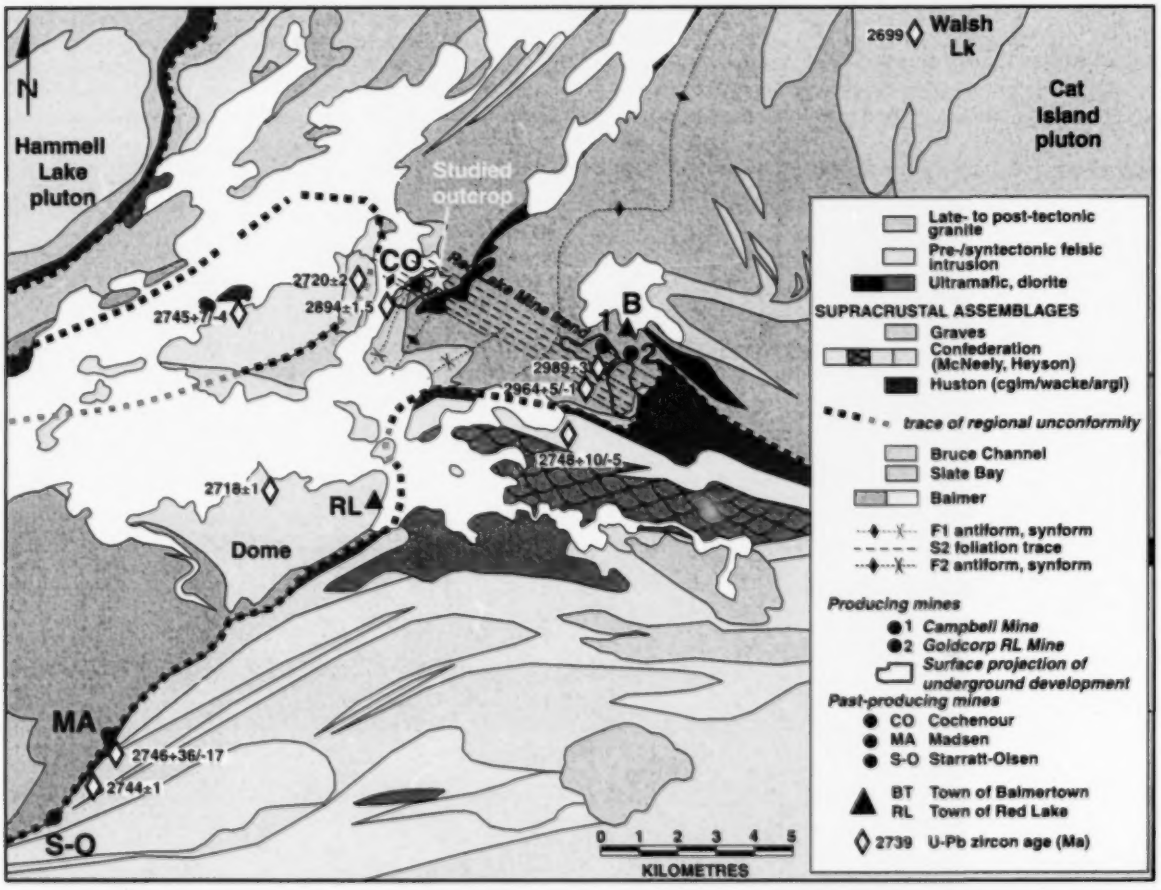

*Figure 1. Geology of Red Lake mine trend area (*modified from *Sanborn-Barrie et al., 2001, and Goldcorp geological data).*

LOCAL GEOLOGICAL SETTING

The geology and gold mineralization of the Cochenour-Willans mine area has been studied by Horwood (1945), Nowlan (1948), Ferguson (1966), Pirie (1982), Andrews et al. (1986), Sanborn (1987), and Hopson (1994), and others. The Cochenour-Willans deposit is hosted by complexly folded, highly altered, massive and pillowed, mafic and ultramafic volcanic rocks and local peridotite intrusions of the Balmer assemblage and associated highly contorted and broken thin (2–5 m) banded chert, argillite, siltstone, and/or iron-formation interflows (Horwood, 1945; Nowlan, 1948; Sanborn, 1987; Hopson, 1994). These rocks are intruded by altered and foliated felsic dykes and post-ore discordant lamprophyre dykes (Horwood, 1945; Nowlan, 1948). Rocks in the Cochenour area are metamorphosed to lower greenschist facies (Sanborn, 1987).

Units in the mine area strike east to northeast and dip steeply south (Horwood, 1945). Horwood (1945) suggested that rock types were deformed by a tight west-plunging (50°) syncline; he indicated that the east-southeast-trending shear zones (130°/50°) hosting most orebodies in the mine coincided with or were subparallel to the syncline axis and that small, high-grade ore shoots plunge 20° to 30°SW. The units and orebodies were subsequently reinterpreted as being located on the south limb of the F_2 Cochenour Anticline, an east-trending fold overturned to the north and plunging 65°W (H.J. Virtanen, T.R. Lloyd, and J.K. MacQueen, unpub. rept., 1989). Most of the gold mineralization is associated with the east-southeast-trending and southwest-dipping D_2 Cochenour shear zone (110°/80°), developed along the south limb and hinge zone of the Cochenour Anticline (H.J. Virtanen, T.R. Lloyd, and J.K. MacQueen, unpub. rept., 1989; Hopson, 1994). Orebodies also occur within metre-wide reverse dextral 'subsidiary shear zones' trending 320° and dipping 60° to 75°SW (Hopson, 1994). These structures, known as '320 structures', hosted the largest and most significant orebodies (Hopson, 1994). They contain metre-wide banded iron-carbonate veins such as the Cochenour main zone and the West Carbonate zone, which have parallel strikes and dip shallowly 30° to 40°SW (Sanborn, 1987). Veins in the West Carbonate zone are confined within highly strained mafic volcanic rocks near the contact with a peridotite intrusion and enclosed within the reverse dextral West Carbonate shear zone (Sanborn, 1987), which strikes 150° to 160° and dips 50°SW. Structures trending 340° to 360°, such as the '04 zone', also host quartz-carbonate veins (H.J. Virtanen, T.R. Lloyd, and J.K. MacQueen, unpub. rept., 1989; Hopson, 1994); they are mineralized where they cut across pyritic black argillite and the pyrite-pyrrhotite-magnetite-rich chert horizon known as the 'main sedimentary facies' (Hopson, 1994).

Hydrothermal alteration is characterized by a strong iron carbonatization with silicification and associated pyrite. Gold mineralization is related to 'cherty' silicification of brecciated quartz-carbonate and massive iron-carbonate veins and replacement zones with associated arsenopyrite, pyrite, sphalerite with local stibnite, pyrrhotite, and chalcopyrite. Small extensional gold-bearing quartz veinlets oriented at high angle to the carbonate bodies also occur locally (Horwood, 1945; Nowlan, 1948; Sanborn, 1987). Iron-carbonate veins such as the West Carbonate zone and the Cochenour main zone are barren (Sanborn, 1987; Hopson, 1994). They constitute the largest and most significant ore zones only where they have been brecciated and silicified or cut by quartz veins.

Ore-zone geometry is extremely complex and disrupted, largely due to progressive ductile-brittle strain, but also to numerous east-southeast, east-, and east-northeast-trending and a few north-trending late to post-ore faults (Horwood, 1945; Sanborn, 1987).

GEOLOGY OF THE COCHENOUR-WILLANS STRIPPED OUTCROP

The Cochenour-Willans stripped outcrop located next to shaft No. 1 has been mapped at a scale of 1:120 (K. Williamson and B. Dubé, work in progress, 2003). Figure 2 shows a simplified version of the map.

Rock types

Altered mafic volcanic rocks and very local interflow volcanic breccia or Balmer assemblage sedimentary rocks are exposed in the stripped outcrop. Several generations of intermediate, mafic to lamprophyre dykes as well as carbonatized and silicified alteration zones and iron-carbonate veins and breccia also occur (Fig. 2).

Mafic volcanic rocks form massive flows and amygdaloidal, foliated, variably altered, and locally variolitic pillow basalt. Pillows are up to 2 m long and moderately flattened. A 40 cm wide interflow of sericitized fine volcaniclastic material or flow breccia trends 223°/64°. Contacts between massive and pillow sequences are poorly exposed because of intense alteration and deformation, although to the southeast, one such contact is sharp, locally marked by a 'black line fault' (*see* below) and crenulated by the S_2 foliation.

Several centimetre- to locally metre-wide, north- and east-trending mafic ('gabbroic') dykes were also mapped. They are foliated and crenulated by S_2 and locally strongly carbonatized.

One vesicular, intermediate dyke oriented 265°/85° cuts across the rocks (Fig. 2). Composed of plagioclase and quartz with amygdales, it is foliated and locally folded by an F_2 fold. It cuts an iron-carbonate breccia vein and is itself locally moderately carbonatized and sericitized. It is thus syn- to late carbonatization and pre- to early D_2 deformation.

Three west-southwest-trending, subvertical (245°/85°), rectilinear, barren lamprophyre dykes are massive, medium grained, and up to 1 m wide. They cut across all rock types, including massive carbonate veins and breccia, as well as the penetrative S_2 foliation, and are known to cut the ore underground (Nowlan, 1947). They exhibit chilled margins (≤12 cm thick) against the basalt and contain green amphibole phenocrysts (approximately 10%; 3–5 mm) in a matrix dominated by feldspar, carbonate, and trace chlorite. Their composition

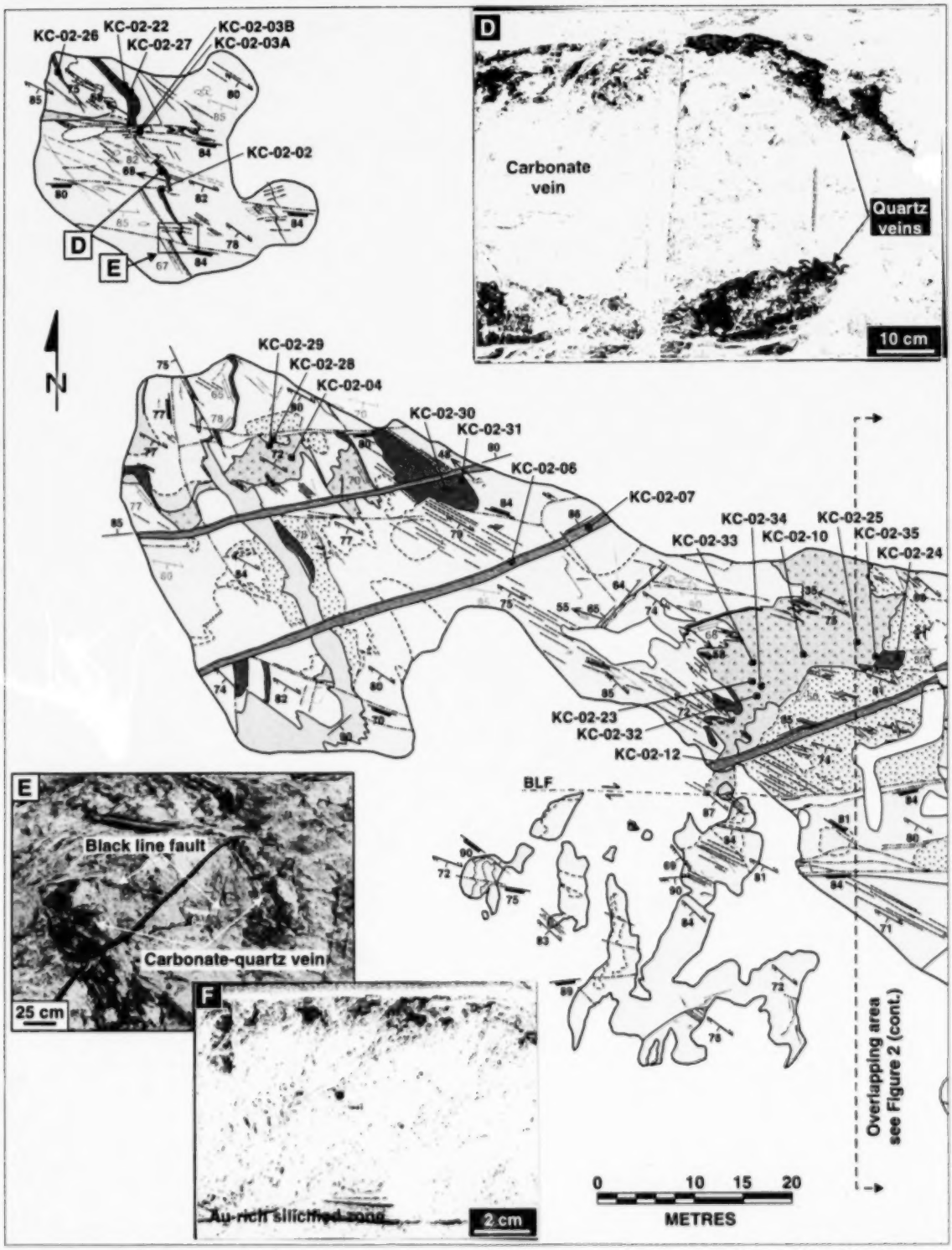

Figure 2. *Detailed geology of the Cochenour stripped outcrop with stereographic projections of the main structural features (equal area projection, lower hemisphere). For clarity, channel samples are not shown. Note the overlap area. D, iron-carbonate quartz vein; E, east-west dextral black line fault cutting an iron-carbonate quartz vein; F, gold-rich silicified zone*

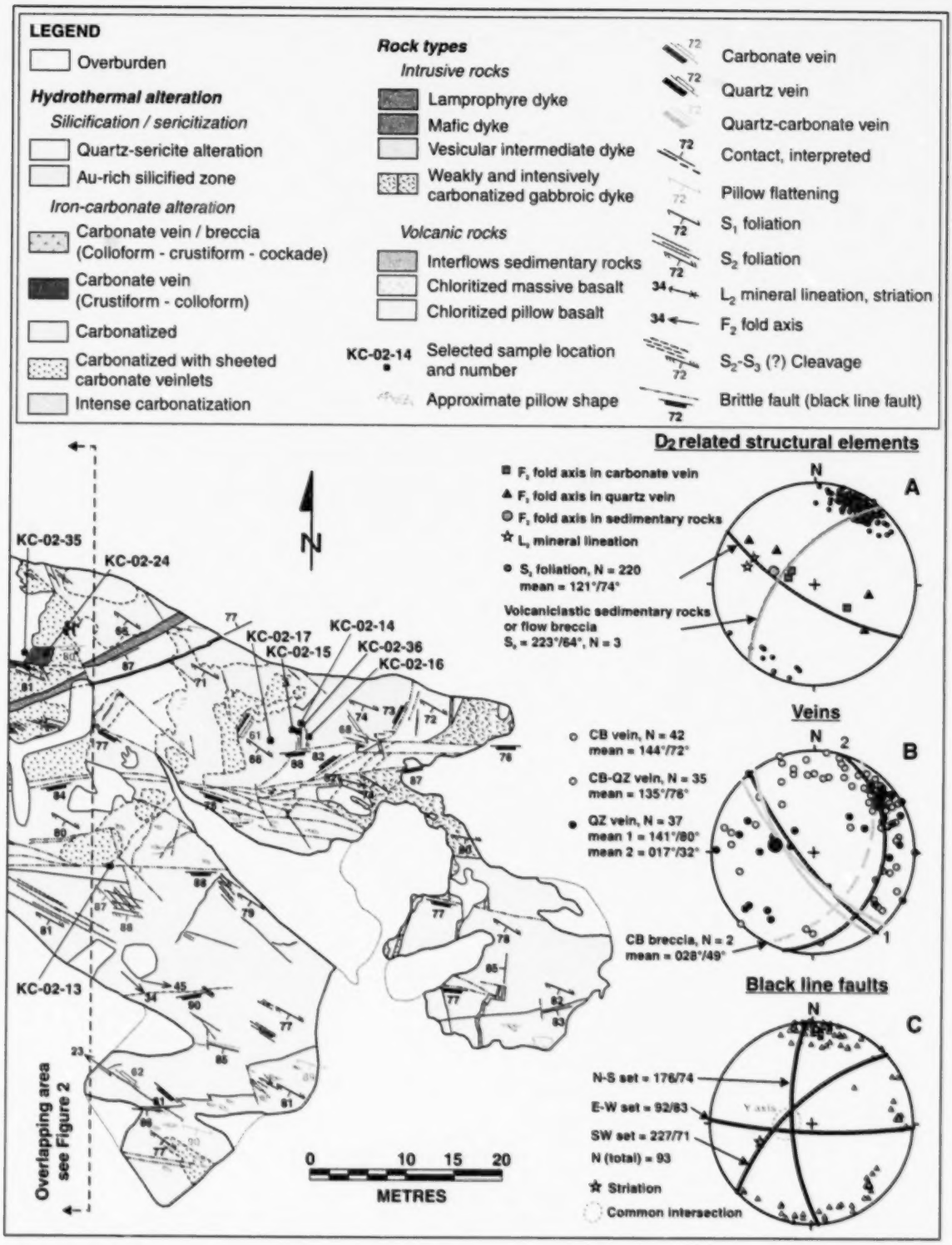

Figure 2 (cont.)

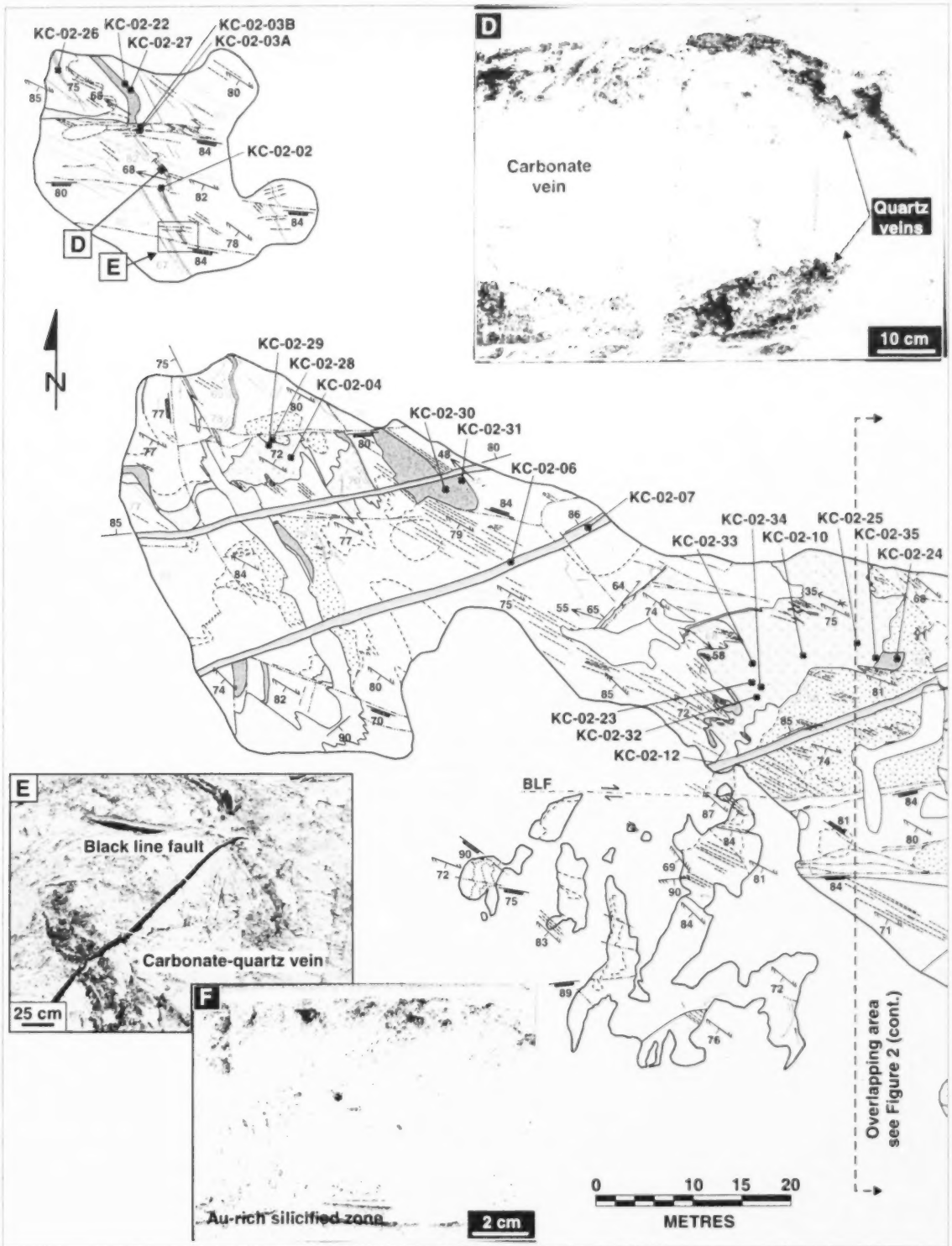

Figure 2. *Detailed geology of the Cochenour stripped outcrop with stereographic projections of the main structural features (equal area projection, lower hemisphere). For clarity, channel samples are not shown. Note the overlap area. D, iron-carbonate quartz vein; E, east-west dextral black line fault cutting an iron-carbonate quartz vein; F, gold-rich silicified zone*

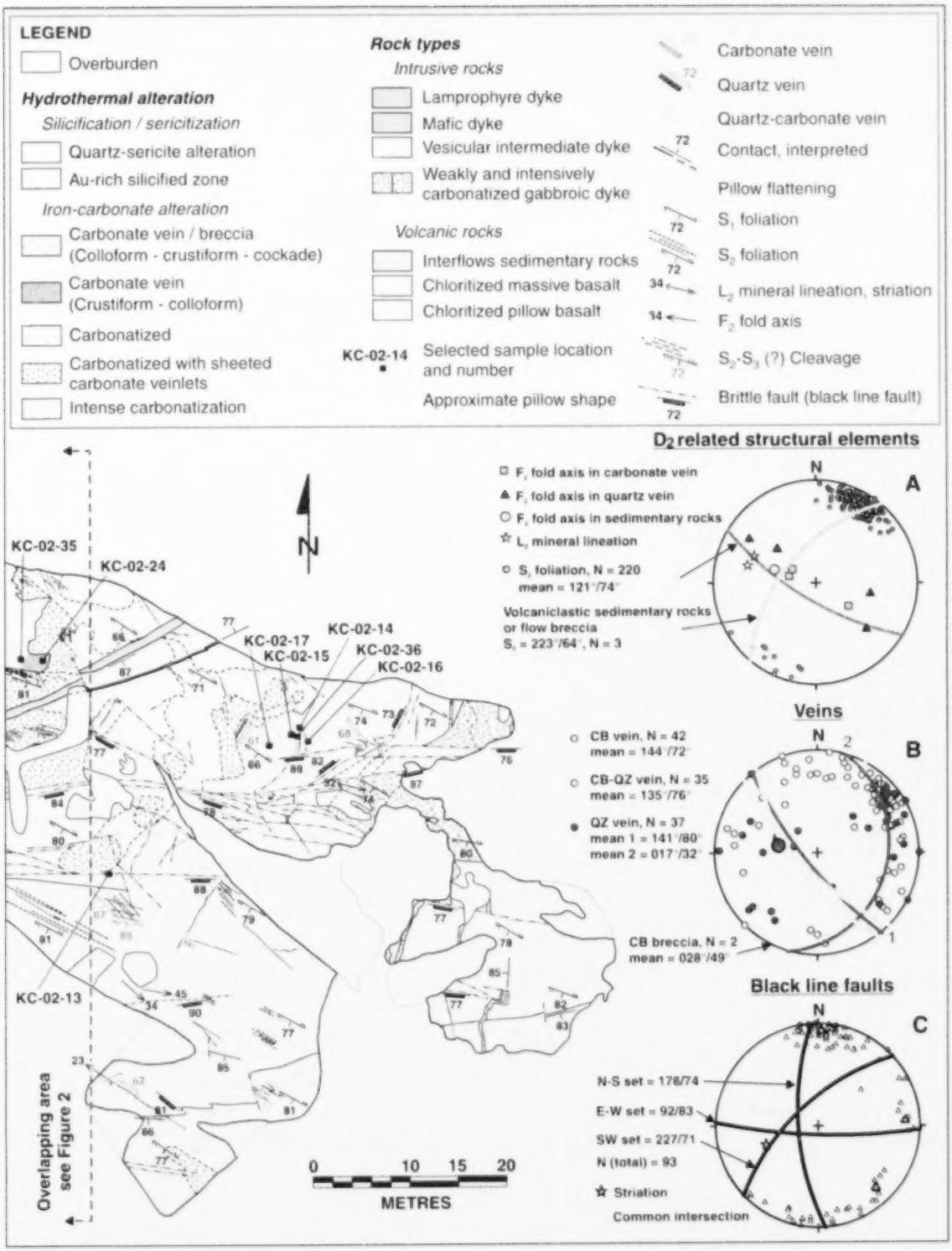

Figure 2 (cont.)

is similar to that of lamprophyre dykes at the Campbell-Red Lake deposit (R. Penczak, pers. comm., 2002; Table 1). Although they clearly cut the massive iron-carbonate veins and breccia, they locally contain an east-southeast-trending foliation (possibly S_2) and are weakly to strongly carbonatized and sericitized, particularly in the central portion where one of them (sample KC-02-12; Table 1) cuts an iron-carbonate breccia. These crosscutting relationships may indicate that several stages of iron-carbonate alteration occurred and that S_2 was locally reactivated (possibly S_3) or that the lamprophyre dykes are syn- to late S_2. The dykes are locally cut by quartz-carbonate veinlets (345°/40°) and extensional quartz veins (025°/45°).

Structure

Sanborn-Barrie et al. (2000,2001) recognized at least two generations of regional structures (D_1, D_2). In the Cochenour area, unit distribution, structures, and an airborne magnetic survey indicate the presence of an open south-southwest-trending F_1 anticline (plunging about 60°S; Nowlan, 1947; Sanborn-Barrie et al., 2000, 2001). The stripped outcrop is located along the north-northeast-trending west limb of this F_1 anticline (Fig. 1).

The nature, orientation, and distribution of the megascopic structural elements were systematically recorded on the large mapped outcrop. S_1 is poorly developed and is clearly visible only in the interflow sedimentary rocks or volcanic breccia where it forms a layer-parallel foliation oriented 220°/64° and crenulated by S_2. The fuchsite-rich clasts within the iron-carbonate breccia also contain an early S_1 fabric crenulated by the main foliation (S_2). Elsewhere, no megascopic evidence of S_1 occurs. The south-southwest-trend of the S_0–S_1 bedding-parallel foliation is compatible with the interpreted geometry of the F_1 anticline.

The outcrop is characterized by a well developed, east-southeast-trending and southwest-dipping S_2 foliation (mean: 121°/74°; Fig. 2a), recorded by all rock types. S_2 is particularly well defined by elongated varioles, vesicules, and amygdales in the pillow basalt and is best developed in the wall rock adjacent to the competent iron-carbonate veins and breccia where it forms a penetrative schistosity enveloping the competent carbonate. Locally, the lamprophyre dykes present weak to moderate foliation oriented 092°/86° to 145°/75° (mean: 121°/77°), which may correlate with S_2 or a younger foliation (possibly S_3). Throughout the outcrop, L_2 stretching lineations are poorly developed and only locally present; they plunge moderately to the west (280°/40°; Fig. 2a). Asymmetric boudinage locally recorded by quartz veinlets injected within an iron-carbonate quartz vein indicates a vertical (possibly reverse) component of movement along the S_2 foliation compatible with L_2.

S_2 foliation is axial planar to local westerly plunging (approximately 50°–70°), northeast-verging F_2 folds that deform the vesicular intermediate dyke and some iron-carbonate and iron-carbonate-quartz veins and breccia (Fig. 2a). In the central part of the outcrop, a 10 to 15 m wide higher strain zone forms a chlorite-carbonate schist in which S_2 is better developed. This zone is characterized by a composite fabric formed by an east-southeast-trending S_2 foliation (mean: 128°/63°) and a slightly oblique fracture cleavage oriented on average 135°/80°. The latter could be a S_2' foliation or a younger cleavage (possibly S_3).

Overall, D_2 strain is moderate with flattened pillows and varioles having an X:Y aspect ratio of ≤3:1. Molar-shaped pillows induced by D_2 strain occur locally (Fig. 3a, b). Their overall shape suggests that the pillowed sequence trends east-northeast (approximately 050–060°) and youngs normally north-northwest. Elsewhere, the pillows are flattened and the flattening plane varies from 090°/75 to 110°/75°, at a slight angle (10°–20°) to the east-souteast-trending S_2 foliation defined by elongated vesicules. The presence of molar-shaped pillows suggests that the outcrop area is within or near the hinge of a F_2 fold.

Late brittle deformation

Late brittle deformation (D_3) is characterized by numerous brittle faults known as 'black line faults' by Red Lake field geologists. Such faults cut many lithological, alteration, vein, and breccia contacts and have significantly added to the complexity of the outcrop (Fig. 2).

Black line faults are discrete, 2 to 4 mm slip planes composed mainly of fine quartz, tourmaline, and dark chlorite. Tourmaline and chlorite are responsible for the typical black colour of these faults and help locate them. Locally, the faults contain quartz with traces of carbonate. They are barren to weakly anomalous in gold (Table 1). Three main sets were found on the outcrop. By far the best developed set trends east and dips steeply south, but some north-, east-northeast-, or south-southeast-trending sets also occur (Fig. 2c). The east-trending sets are dextral with displacement over centimetres to several metres; the north- and east-southeast-trending sets are sinistral. In the northwestern part of the outcrop, an east-trending, metre-wide black-line-fault corridor cuts and dextrally displaces an iron-carbonate quartz vein. It contains several D and synthetic R Riedel-type brittle faults that are compatible with dextral displacement (Fig. 2).

The black line faults cut the iron-carbonate veins and breccia and the carbonate-quartz veins (Fig. 2e). They also displace the auriferous silicified alteration zone over 50 m in the eastern part of the map area (Fig. 2). Lamprophyre dykes are locally cut by north- to south-southeast-trending black line faults, showing an apparent sinistral displacement over less than 1 m. Some southwest-trending (230°/78°) black line faults are locally crenulated by the east-southeast-trending foliation, suggesting that the faults are late D_2 or most probably that the S_2 foliation was re-activated following formation of the faults.

Hydrothermal alteration, veining, and mineralization

The stripped outcrop contains exposures of iron-carbonate veins and breccia with spectacular colloform-crustiform and cockade textures as well as a high-grade, auriferous, silicified

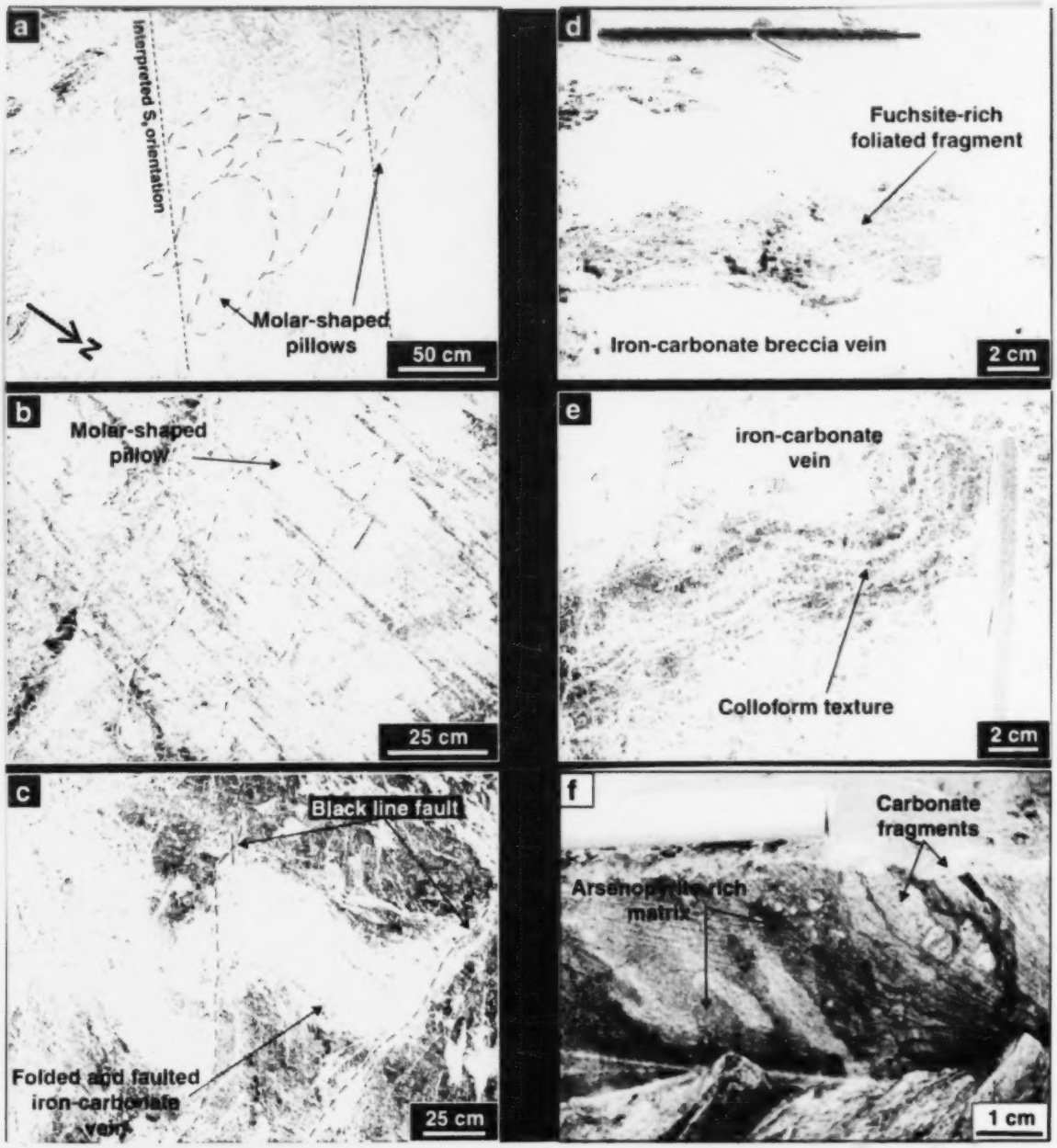

Figure 3. *a) Molar-shaped pillows; b) molar-shaped pillow; c) crustiform iron-carbonate vein folded by F_2 and cut by black line faults; d) foliated (S_2) fuchsite-rich clasts in iron-carbonate breccia; e) colloform texture in iron-carbonate breccia; f) brecciated and arsenopyrite-rich iron-carbonate vein.*

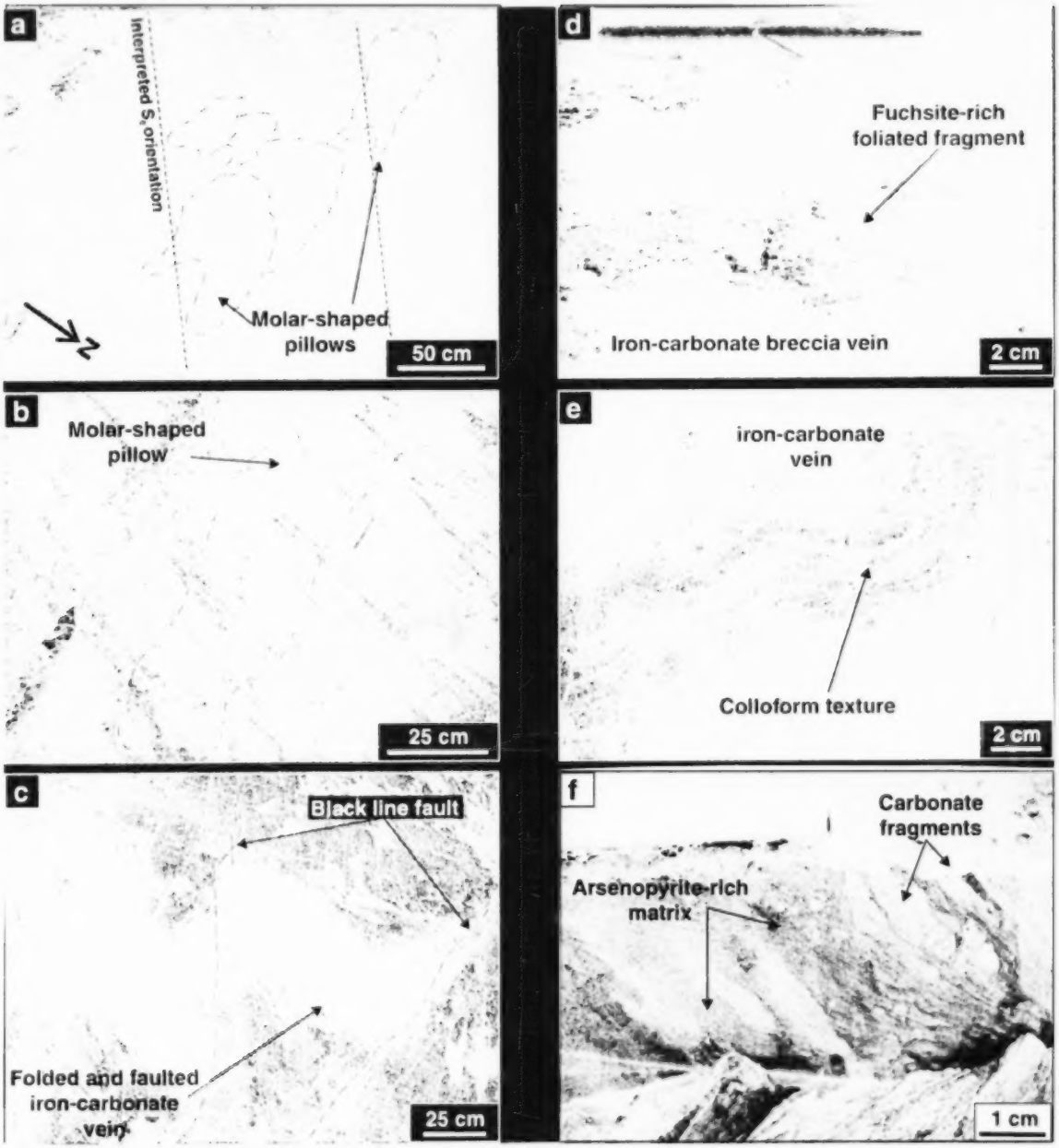

Figure 3. *a) Molar-shaped pillows; b) molar-shaped pillow; c) crustiform iron-carbonate vein folded by F_2 and cut by black line faults; d) foliated (S_2) fuchsite-rich clasts in iron-carbonate breccia; e) colloform texture in iron-carbonate breccia; f) brecciated and arsenopyrite-rich iron-carbonate vein*

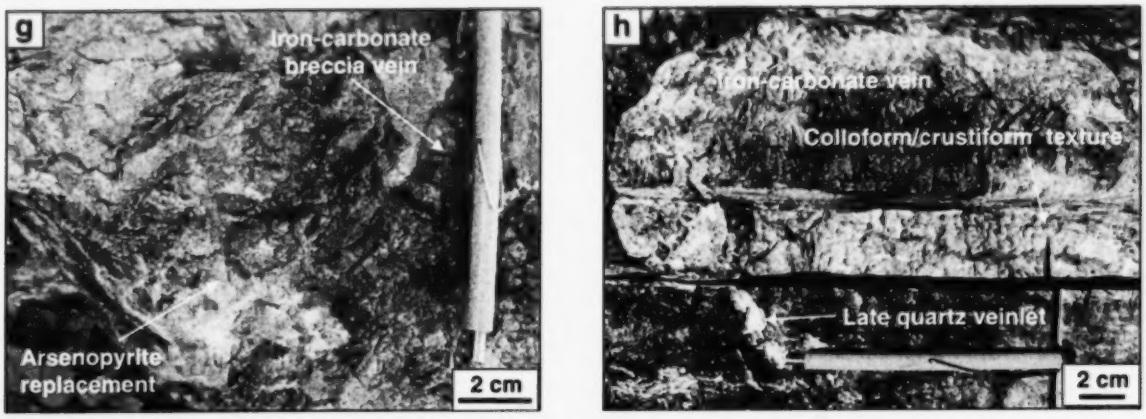

Figure 3. g) arsenopyrite in iron-carbonate vein; h) colloform texture in gold-rich iron-carbonate vein (sample KC-02-31).

zone. The host mafic volcanic rocks are locally strongly altered; several alteration assemblages can be mapped (Fig. 2). However, the original distribution of the rocks, alteration zones, and veins has been significantly modified by numerous post-mineralization black line faults.

Iron-carbonate alteration and veining

Iron-carbonate (ankerite) veining and replacement is the dominant type of hydrothermalism. Several massive ankerite veins up to 70 cm wide occur in the outcrop. A carbonate-quartz vein (Fig. 2e) in the northwestern part of the outcrop is oriented 135°/74° and is at a slight angle to the S_2 foliation (Fig. 2b). To the east, the vein is folded by F_2 and crosscut by black line faults. The vein is up to 1 m wide and corresponds to an extensional vein composed of massive carbonate and local ankerite fibres perpendicular to the walls with traces of disseminated quartz. It is cut by extensional barren quartz veins (≤15–20 cm wide) with traces of carbonate that are injected symmetrically along its margins (Fig. 2d) and by multiple sets of barren extensional quartz veinlets in its central part. Such quartz veins are barren of gold (Table 1). The immediate wall rock of the iron-carbonate vein also contains sheeted extensional quartz veins oriented 130°/70°, subparallel to the carbonate-quartz vein. They clearly postdate iron-carbonate veining and were injected along the margins of the carbonate vein because of competence contrast with the host basalt (Fig. 2e).

Two spectacular iron-carbonate zones 8 to 10 m wide are exposed in the outcrop (Fig. 2). They consist of large iron-carbonate breccia, centimetre-wide, north-northeast-trending, massive extensional carbonate veins with ankerite fibres at high angles to vein walls, and local massive iron-carbonate replacement zones. They are cut by a local stockwork of barren quartz veinlets. Their envelope trends north-northeast (028°/49°) at a high angle to S_2 (Fig. 2b). The iron-carbonate breccia contains foliated (S_2) wall-rock clasts characterized by green mica (fuchsite), with carbonate, quartz, and rutile or leucoxene (Fig. 3d). Clast foliation is subparallel to the S_2 fabric outside the breccia, suggesting that this foliation postdates carbonate brecciation and veining. S_2 foliation is also weakly developed in the carbonate matrix. One of the two iron-carbonate breccia units presents spectacular examples of cockade, colloform, and crustiform textures typical of a low-sulphidation epithermal systems (Fig. 3e). The occurrence of fuchsite-rich carbonatized and silicified clasts within the breccia veins suggests that these iron-carbonate zones probably developed within two small basaltic komatiite interflows within the basalt. The relatively high Cr (534 ppm) and Ni (377 ppm) content in one fuchsite-rich breccia sample is compatible with such an interpretation (Table 1). Their north-northeast orientation could define the layering–bedding trace in the host sequence pre-D_2 deformation. This is compatible with the north-northeast orientation suggested by the trend of the molar-shaped pillows, with the interflow unit (Fig. 2a, b), and with the trend of units defined by regional mapping and geophysics (Fig. 1).

Traces to a few percentages of fine pyrite occur locally in the iron-carbonate veins and breccia and associated wall rock. Overall, the massive iron-carbonate veins and breccia contain low-grade gold mineralization, typically ≤1 to 2 g/t Au, and very limited arsenic and sulphur; the injected whitish quartz veinlets are also barren of to anomalous in gold. Table 1 presents results from analyses and illustrates the low gold content of these iron-carbonate veins and breccia. The CO_2, MgO, Fe_2O_3, and SiO_2 concentrations indicate that the veins are dominated by ankerite, although they also contain some quartz.

Significant gold mineralization with up to 31 g/t Au over 0.3 m and 6.9 g/t Au over 3.5 m, including 17 g/t Au over 0.6 m, was found in channels in some iron-carbonate veins and breccia, including those with colloform-crustiform texture (Goldcorp Inc., unpub. rept., 1998). Table 1 illustrates the abundance of arsenic with SiO_2 and sulphur and varied proportions of antimony in most significant gold mineralization hosted by the iron-carbonate veins and breccia analyzed

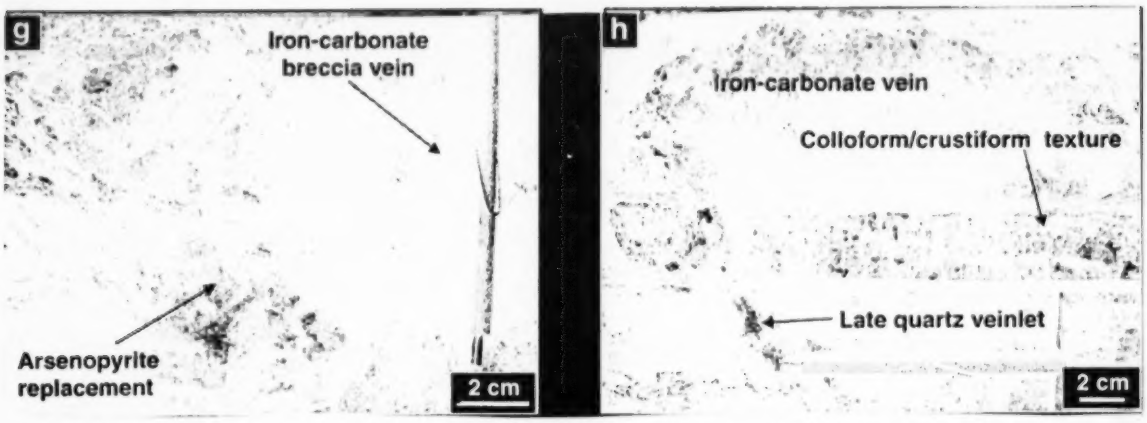

Figure 3. *g) arsenopyrite in iron-carbonate vein;* ***h)*** *colloform texture in gold-rich iron-carbonate vein (sample KC-02-31).*

zone. The host mafic volcanic rocks are locally strongly altered; several alteration assemblages can be mapped (Fig. 2). However, the original distribution of the rocks, alteration zones, and veins has been significantly modified by numerous post-mineralization black line faults.

Iron-carbonate alteration and veining

Iron-carbonate (ankerite) veining and replacement is the dominant type of hydrothermalism. Several massive ankerite veins up to 70 cm wide occur in the outcrop. A carbonate-quartz vein (Fig. 2e) in the northwestern part of the outcrop is oriented 135°/74° and is at a slight angle to the S_2 foliation (Fig. 2b). To the east, the vein is folded by F_2 and crosscut by black line faults. The vein is up to 1 m wide and corresponds to an extensional vein composed of massive carbonate and local ankerite fibres perpendicular to the walls with traces of disseminated quartz. It is cut by extensional barren quartz veins (≤15–20 cm wide) with traces of carbonate that are injected symmetrically along its margins (Fig. 2d) and by multiple sets of barren extensional quartz veinlets in its central part. Such quartz veins are barren of gold (Table 1). The immediate wall rock of the iron-carbonate vein also contains sheeted extensional quartz veins oriented 130°/70°, subparallel to the carbonate-quartz vein. They clearly postdate iron-carbonate veining and were injected along the margins of the carbonate vein because of competence contrast with the host basalt (Fig. 2e).

Two spectacular iron-carbonate zones 8 to 10 m wide are exposed in the outcrop (Fig. 2). They consist of large iron-carbonate breccia, centimetre-wide, north-northeast-trending, massive extensional carbonate veins with ankerite fibres at high angles to vein walls, and local massive iron-carbonate replacement zones. They are cut by a local stockwork of barren quartz veinlets. Their envelope trends north-northeast (028°/49°) at a high angle to S_2 (Fig. 2b). The iron-carbonate breccia contains foliated (S_2) wall-rock clasts characterized by green mica (fuchsite), with carbonate, quartz, and rutile or leucoxene (Fig. 3d). Clast foliation is subparallel to the S_2 fabric outside the breccia, suggesting that this foliation postdates carbonate brecciation and veining. S_2 foliation is also weakly developed in the carbonate matrix. One of the two iron-carbonate breccia units presents spectacular examples of cockade, colloform, and crustiform textures typical of a low-sulphidation epithermal systems (Fig. 3e). The occurrence of fuchsite-rich carbonatized and silicified clasts within the breccia veins suggests that these iron-carbonate zones probably developed within two small basaltic komatiite interflows within the basalt. The relatively high Cr (534 ppm) and Ni (377 ppm) content in one fuchsite-rich breccia sample is compatible with such an interpretation (Table 1). Their north-northeast orientation could define the layering–bedding trace in the host sequence pre-D_2 deformation. This is compatible with the north-northeast orientation suggested by the trend of the molar-shaped pillows, with the interflow unit (Fig. 2a, b), and with the trend of units defined by regional mapping and geophysics (Fig. 1).

Traces to a few percentages of fine pyrite occur locally in the iron-carbonate veins and breccia and associated wall rock. Overall, the massive iron-carbonate veins and breccia contain low-grade gold mineralization, typically ≤1 to 2 g/t Au, and very limited arsenic and sulphur; the injected whitish quartz veinlets are also barren of to anomalous in gold. Table 1 presents results from analyses and illustrates the low gold content of these iron-carbonate veins and breccia. The CO_2, MgO, Fe_2O_3, and SiO_2 concentrations indicate that the veins are dominated by ankerite, although they also contain some quartz.

Significant gold mineralization with up to 31 g/t Au over 0.3 m and 6.9 g/t Au over 3.5 m, including 17 g/t Au over 0.6 m, was found in channels in some iron-carbonate veins and breccia, including those with colloform-crustiform texture (Goldcorp Inc., unpub. rept., 1998). Table 1 illustrates the abundance of arsenic with SiO_2 and sulphur and varied proportions of antimony in most significant gold mineralization hosted by the iron-carbonate veins and breccia analyzed

Table 1. Major- and trace-element chemistry of the main elements.

	SiO_2[1] %	Al_2O_3[1] %	TiO_2[1] %	CaO[1] %	MgO[1] %	Na_2O[1] %	K_2O[1] %	Fe_2O_3[1] %	MnO[1] %	LOI[1] %	Sum %	S[7] %	CO_2[6] %	Au[5] ppb	As[2,4] ppm	Sb[4] ppm	Ag[2] ppm	Cu[2] ppm	Zn[2] ppm	Y[1] ppm	Zr[1] ppm	Sc[2] ppm	Cr[2] ppm	V[2] ppm	Ni[2] ppm	B[3] ppm
Iron-carbonate colloform-crustiform vein/breccia																										
KC-02-02A	18.15	0.09	<0.01	25.56	15.81	<0.01	0.02	3.45	0.13	37.25	100.47	<0.01	37.9	180	2.1	2.5	1.0	4.3	29.3	4	14	0.9	5	33	4	12
KC-02-10	2.48	0.41	0.04	30.23	17.91	0.03	0.07	5.21	0.17	43.85	100.46	<0.01	45	241	129	3.9	1.1	2.1	15.8	5	7	1.4	2	12	6	<10
KC-02-24	6.18	0.44	0.02	29.22	17.19	<0.01	0.07	5.25	0.19	41.7	100.28	<0.01	42.7	46	27.3	1.8	1.2	2.5	49	5	8	2.5	3	13	8	18
KC-02-26	21.16	1.99	0.11	23.38	12.23	<0.01	0.48	7.4	0.24	33.3	100.29	<0.01	33.1	698	160	8.4	1	11.2	25.6	6	18	7.2	13	71	14	<10
KC-02-28	7.47	0.13	0.01	28.94	17.23	<0.01	0.02	4.6	0.17	41.8	100.38	<0.01	42.4	272	18.6	1.9	1.1	1.3	24.5	5	9	3.1	4	11	7	31
KC-02-29	18.03	1.39	0.07	24.86	14.74	0.02	0.3	5.31	0.17	35.65	100.58	0.01	34.9	674	311	18.2	1.1	9.7	24.2	6	12	8.7	30	40	21	93
KC-02-30	3.33	0.3	0.03	30	17.66	<0.01	0.05	5.64	0.19	43.2	100.38	<0.01	44.9	197	49.6	2.1	1.1	3.4	20.2	5	6	3	2	11	9	113
KC-02-33	11.05	0.84	0.07	27.1	15.31	<0.01	0.16	6.31	0.19	39.2	100.27	0.04	40.1	242	307	5.3	1.1	4.6	18.5	8	6	2.6	5	27	13	<10
Mineralized iron-carbonate vein (brecciated)																										
KC-02-22	43.65	3.04	0.2	16.18	9.57	0.04	0.66	5.74	0.15	21	100.27	0.63	23.6	3090	4770	58	0.9	19.3	31.1	9	19	9.5	27	76	24	13
KC-02-23	4.07	0.7	0.07	29.46	17.62	<0.01	0.11	5.11	0.17	43	100.27	0.05	44.8	2610	1250	9.5	1.2	2.5	19.8	4	8	3.2	6	23	9	48
KC-02-25	15.44	5.41	0.48	24.03	13.77	0.12	1.06	6.25	0.18	33.6	100.36	0.61	33.6	857	2590	57.4	1.8	55.6	24.9	12	27	15.7	23	125	21	25
KC-02-27	27.72	5.46	0.53	18.51	10.56	0.14	1.14	9.29	0.24	23	96.62	2.16	26.3	10000	6410	107	1.3	38.4	36.1	18	37	17.2	29	133	69	51
KC-02-31	11.48	0.97	0.1	27.12	16.68	0.02	0.2	4.4	0.16	39.4	100.57	<0.01	38.7	22800	109	4.2	1.8	7.7	16.1	4	10	3	6	29	7	128
KC-02-32	20.32	4.82	0.44	22.66	13.73	0.15	1.07	5.22	0.14	31.55	100.16	0.46	32.8	10100	3720	24	1.2	20.2	15.7	11	26	15.2	33	113	26	19
KC-02-34	2.26	0.05	<0.01	30.41	18.62	<0.01	0.02	4.26	0.15	44.65	100.38	<0.01	44.8	3770	453	3	1	0.8	12.1	5	4	0.5	<1	6	3	<10
KC-02-35	31.12	6.68	0.61	16.2	10.21	0.19	1.57	6.88	0.14	21.4	95.03	1.8	24.2	33400	8750	105	2	73.8	19.7	16	35	19.3	30	152	39	19
Fuchsite-rich clasts in carbonate breccia vein																										
KC-02-04	57.86	7.95	0.41	8.8	5.5	0.19	1.66	4.59	0.09	13.1	100.21	0.41	13	67	969	218	0.4	90.4	52.6	12	31	19.8	534	122	377	253
Barren quartz vein injected along walls of iron-carbonate vein																										
KC-02-02B	91.2	0.52	<0.01	2.57	1.47	<0.01	0.11	0.84	0.03	3.55	100.2	<0.01	3.69	7	10.4	14	<0.2	8.4	16.8	4	3	0.6	6	6	4	88
Au-rich silicified zone																										
KC-02-14	79.24	8.32	0.39	0.05	0.14	0.16	2.16	5.12	<0.01	4.6	100.17	2.89	<0.01	11500	>10000	206	0.7	41	9.3	9	26	6.7	89	142	91	48
KC-02-15	74.01	6.59	0.32	0.13	0.14	0.18	1.55	9.54	<0.01	7.95	100.4	5.74	<0.01	58000	>10000	101	1.8	42.5	12	8	16	5.5	38	94	74	186
KC-02-16	90.3	2.05	0.06	1.15	0.92	0.05	0.49	2.76	0.02	2.25	100.08	0.83	1.59	386300	>10000	188	>10	293	33.3	2	8	2.4	11	30	22	67
KC-02-17A	74.97	10.2	1.31	0.21	0.17	0.37	2.55	5.1	<0.01	5.1	100.09	3.12	0.05	3400	>10000	120	0.5	34.5	7.8	19	86	6.1	32	191	78	58
KC-02-36	78.79	5.79	0.26	0.15	0.14	0.08	1.43	7.17	<0.01	6.4	100.3	4.17	0.11	62100	>10000	80.8	2	39.9	8.2	9	17	4.9	38	84	60	134
"Black line fault"																										
KC-02-03A	45.62	11.3	1.3	9.53	5.27	0.19	1.47	12.1	0.27	13.1	100.26	0.6	12.5	161	281	44.9	0.5	95	123	27	85	32	17	302	36	452
KC-02-03B	44.96	12.4	1.39	7.43	5.55	0.1	1.12	15.5	0.26	11.25	100.05	0.3	9.21	29	52.7	31.9	0.4	38.4	175	27	95	33.9	18	294	37	22
KC-02-13	61.64	11.6	0.49	2.5	4.88	0.15	0.66	12.58	0.22	5.5	100.25	0.27	2.81	18	37.1	7.2	0.2	22.3	98.5	9	33	29.8	70	211	72	112
Lamprophyre dyke (*=altered dyke)																										
KC-02-06	49.59	12.9	0.63	7.5	6.69	3.73	0.35	7.96	0.12	10.5	99.99	0.16	9.31	<1	11.5	52.3	0.4	79.9	72.2	12	117	16.2	318	117	139	<10
KC-02-07	47.88	12.1	0.61	8.89	7.3	3.46	0.08	7.95	0.13	10.7	99.2	0.13	10.1	<1	8.9	49.9	0.3	71	69	11	109	17.4	335	116	154	<10
KC-02-12*	58.3	16.3	0.76	7.82	1.53	0.73	3.24	3.67	0.05	7.4	100.01	1.23	7.41	32	28.1	58.1	0.3	68.2	22.6	10	164	3.7	7	50	12	13

Analysis by XRAL Laboratories: 1=X-ray fluorescence spectrometry, 2=ICP-80, 3=ICP90A, 4=Fusion/ICP/Hybrid AA, 5=Fire assay (gravimetric finish), 6=Coulometry, 7=Leco;
LOI, Loss on ignition.

in this study. Base-metal and silver concentrations are very limited. Petrographic work indicates that most auriferous zones correspond either to massive extensional ankerite veins cut by small arsenopyrite veinlets (≤0.5 mm), or to brecciated ankerite veins with ≤1 cm wide, semi-massive, fine arsenopyrite and coarser grained pyrite with leucoxene or anatase and sericite and varied proportions of carbonate. The gold mineralization in the iron-carbonate veins and breccia is thus related to brecciation and associated silicification, and fine arsenopyrite postdating iron-carbonate deposition (Fig. 3f, g). Similar relationships underground were described by Sanborn (1987). The only exception is sample KC-02-31 from a colloform-crustiform massive ankerite vein that contains 22.8 ppm Au and has no significant megascopic and petrographic evidence of brecciation, silicification, and arsenic and sulphur (Table 1; Fig. 3h). Similar results from this vein were reported by Inco (unpub. rept., 1989). Gold is probably related to the local presence of small auriferous quartz veinlets as described underground (Horwood, 1945; Sanborn, 1987).

The altered rocks adjacent to iron-carbonate veins and breccia are barren and commonly characterized by rusty weathering that is related to intense iron-carbonate replacement over tens of centimetres to a few metres with varied proportions of sericite and chlorite (≤10–20%). They contain traces of sulphides with only anomalous gold values (≤1 g/t gold). They are locally injected by sheeted extensional carbonate veinlets that commonly have been crenulated and/or transposed by S_2. Farther away from the iron-carbonate veins and breccia, carbonatization intensity decreases and the alteration is dominated by chlorite, giving a greenish colour to the weathered surface. This chlorite-dominated alteration zone generally contains less than 5 to 10% iron carbonate and dominates the eastern to southeastern portions of the outcrop.

Auriferous silicified zone

The main auriferous zone exposure corresponds to a metre-wide 'bleached' alteration zone characterized by silicification ('silica flooding'), with varied proportions of sericite and/or green mica occurring mainly in foliated wall-rock clasts or remnants, and traces of carbonate. The silicified zone is commonly massive, light grey, and featureless (Fig. 2f), although it is locally brecciated and records S_2. It contains up to 90% SiO_2 with varied proportions of Al_2O_3 and K_2O (Table 1). Most if its contacts, especially the eastern one, are marked by black line faults. Quartz is very fine grained and recrystallized. The nature of the protolith is difficult to determine because of the intensity of the silicification. Local subparallel layering in amygdaloidal feldspar- and quartz-rich rocks could represent preserved flow banding and indicate an intermediate to felsic protolith. Alternatively, the presence of green mica may suggest that the unit is a strongly bleached and silicified mafic-ultramafic unit, which is compatible with its very low Y and Zr contents (Table 1).

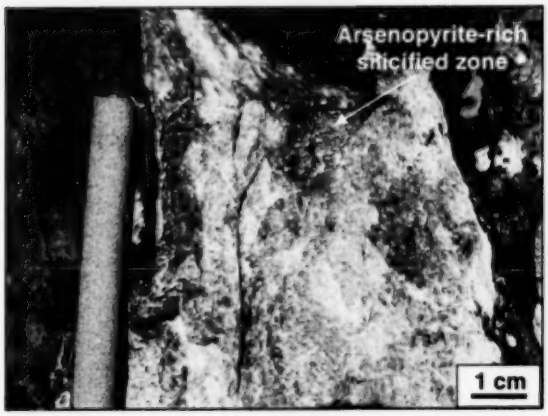

Figure 4. *Disseminated fine arsenopyrite in gold-rich silicified zone.*

The silicified alteration zone is cut by up to 10 to 20% irregular quartz veins and veinlets and by local, north-trending, steeply dipping, en échelon quartz veinlets. Overall, it contains traces to a few percentages of sulphides. However, gold-bearing zones are medium grey and contain 5 to 20% sulphides, mainly fine arsenopyrite with pyrite in fine-grained quartz (Fig. 4). Sulphides are commonly spatially associated with aggregates of TiO_2-bearing minerals (rutile, leucoxene, anatase) and traces of tourmaline in irregular bands or veinlets cutting across the quartz-rich matrix.

Gold values in channels reported by Inco (unpub. rept., 1989) reach 143 g/t Au over 1 m. Channel sampling by Goldcorp intersected values reaching 41 g/t Au over 5.5 m (Goldcorp Inc., unpub. rept., 1998). Two visible gold grains were found, one in the silicic replacement and the other in a quartz veinlet. Under the microscope, gold occurs as fracture fillings in pyrite. Our analyses show high-grade gold values associated with abundant arsenic and sulphide, with very limited base metals, silver, antimony, and CO_2 (Table 1). They clearly illustrate the relationships between silica replacement, with associated arsenopyrite, and high gold concentration.

The auriferous silicified zone is cut by black line faults with an apparent dextral displacement of approximately 50 m (Fig. 2).

A greenish sericite-silicic alteration zone with some iron-carbonate forms the proximal envelope to the gold-rich silicified zone. Local varioles and/or amygdales are preserved within this zone and indicate a pillow basalt protolith. The gradual transition between this sericite-silicic alteration and the auriferous silicic mineralized zone suggests that the auriferous-zone protolith could also be, at least in part, a variolitic basalt. However, as most contacts are marked by black line faults, the nature of the protolith is difficult, if not impossible, to determine on the basis of an apparent gradual transition between these altered and bleached zones, as their activation postdates alteration.

in this study. Base-metal and silver concentrations are very limited. Petrographic work indicates that most auriferous zones correspond either to massive extensional ankerite veins cut by small arsenopyrite veinlets (≤0.5 mm), or to brecciated ankerite veins with ≤1 cm wide, semi-massive, fine arsenopyrite and coarser grained pyrite with leucoxene or anatase and sericite and varied proportions of carbonate. The gold mineralization in the iron-carbonate veins and breccia is thus related to brecciation and associated silicification, and fine arsenopyrite postdating iron-carbonate deposition (Fig. 3f, g). Similar relationships underground were described by Sanborn (1987). The only exception is sample KC-02-31 from a colloform-crustiform massive ankerite vein that contains 22.8 ppm Au and has no significant megascopic and petrographic evidence of brecciation, silicification, and arsenic and sulphur (Table 1; Fig. 3h). Similar results from this vein were reported by Inco (unpub. rept., 1989). Gold is probably related to the local presence of small auriferous quartz veinlets as described underground (Horwood, 1945; Sanborn, 1987).

The altered rocks adjacent to iron-carbonate veins and breccia are barren and commonly characterized by rusty weathering that is related to intense iron-carbonate replacement over tens of centimetres to a few metres with varied proportions of sericite and chlorite (≤10–20%). They contain traces of sulphides with only anomalous gold values (≤1 g/t gold). They are locally injected by sheeted extensional carbonate veinlets that commonly have been crenulated and/or transposed by S_2. Farther away from the iron-carbonate veins and breccia, carbonatization intensity decreases and the alteration is dominated by chlorite, giving a greenish colour to the weathered surface. This chlorite-dominated alteration zone generally contains less than 5 to 10% iron carbonate and dominates the eastern to southeastern portions of the outcrop.

Auriferous silicified zone

The main auriferous zone exposure corresponds to a metre-wide 'bleached' alteration zone characterized by silicification ('silica flooding'), with varied proportions of sericite and/or green mica occurring mainly in foliated wall-rock clasts or remnants, and traces of carbonate. The silicified zone is commonly massive, light grey, and featureless (Fig. 2f), although it is locally brecciated and records S_2. It contains up to 90% SiO_2 with varied proportions of Al_2O_3 and K_2O (Table 1). Most if its contacts, especially the eastern one, are marked by black line faults. Quartz is very fine grained and recrystallized. The nature of the protolith is difficult to determine because of the intensity of the silicification. Local subparallel layering in amygdaloidal feldspar- and quartz-rich rocks could represent preserved flow banding and indicate an intermediate to felsic protolith. Alternatively, the presence of green mica may suggest that the unit is a strongly bleached and silicified mafic-ultramafic unit, which is compatible with its very low Y and Zr contents (Table 1).

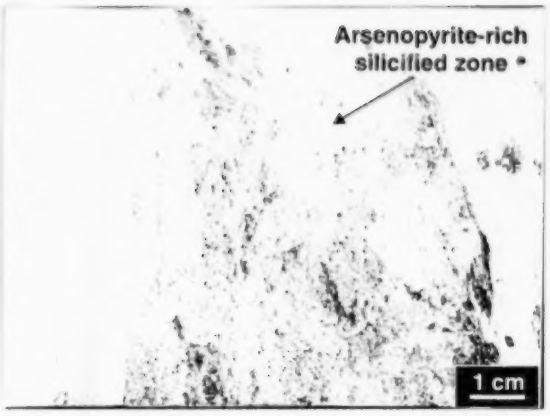

Figure 4. *Disseminated fine arsenopyrite in gold-rich silicified zone.*

The silicified alteration zone is cut by up to 10 to 20% irregular quartz veins and veinlets and by local, north-trending, steeply dipping, en échelon quartz veinlets. Overall, it contains traces to a few percentages of sulphides. However, gold-bearing zones are medium grey and contain 5 to 20% sulphides, mainly fine arsenopyrite with pyrite in fine-grained quartz (Fig. 4). Sulphides are commonly spatially associated with aggregates of TiO_2-bearing minerals (rutile, leucoxene, anatase) and traces of tourmaline in irregular bands or veinlets cutting across the quartz-rich matrix.

Gold values in channels reported by Inco (unpub. rept., 1989) reach 143 g/t Au over 1 m. Channel sampling by Goldcorp intersected values reaching 41 g/t Au over 5.5 m (Goldcorp Inc., unpub. rept., 1998). Two visible gold grains were found, one in the silicic replacement and the other in a quartz veinlet. Under the microscope, gold occurs as fracture fillings in pyrite. Our analyses show high-grade gold values associated with abundant arsenic and sulphide, with very limited base metals, silver, antimony, and CO_2 (Table 1). They clearly illustrate the relationships between silica replacement, with associated arsenopyrite, and high gold concentration.

The auriferous silicified zone is cut by black line faults with an apparent dextral displacement of approximately 50 m (Fig. 2).

A greenish sericite-silicic alteration zone with some iron-carbonate forms the proximal envelope to the gold-rich silicified zone. Local varioles and/or amygdales are preserved within this zone and indicate a pillow basalt protolith. The gradual transition between this sericite-silicic alteration and the auriferous silicic mineralized zone suggests that the auriferous-zone protolith could also be, at least in part, a variolitic basalt. However, as most contacts are marked by black line faults, the nature of the protolith is difficult, if not impossible, to determine on the basis of an apparent gradual transition between these altered and bleached zones, as their activation postdates alteration.

DISCUSSION

The stripped outcrop examined in this study shows several features described from underground work at the mine. The large iron-carbonate zones share characteristics with the north-south '04 structures'; the carbonate-quartz vein trending 135/74° is subparallel to the east-southeast trend reported by Horwood (1945) and could also correspond to the '320' structure (West Carbonate zone), whereas the S_2 foliation is subparallel to the fabric in the Cochenour shear. The exposed geological setting also has characteristics in common with the Campbell-Red Lake deposit (Penczak and Mason, 1997; Dubé et al., 2002). The cockade, colloform-crustiform textures in the iron-carbonate veins and breccia are typical of the barren carbonate veins underground at the Cochenour-Willans mine (Sanborn , 1987) and in the Goldcorp High Grade zone (Dubé et al., 2001a, 2002), and both are hosted in Balmer assemblage pillow basalt. Metamorphic grade is lower (greenschist) than at the Red Lake mine (lower amphibolite).

The ankerite breccia veins with fuchsite-rich clasts may be confined within ultramafic interflows, as suggested by abundant fuchsite and relatively high nickel and chromium contents. They share some characteristics with the highly carbonatized and veined basaltic komatiite adjacent to the ore zone in the Campbell-Red Lake deposit (Penczak and Mason, 1997; Dubé et al., 2002). However, due to post-alteration black line faulting, the original geometry and geological parameters controlling the formation and timing of the ankerite breccia veins and auriferous silicified zone are difficult to define. Most alteration zones, carbonate breccia, carbonate-quartz veins, and gold-rich silicified zones are at a high angle to and/or are crenulated or folded by S_2, suggesting that they are pre- to early D_2 deformation. The north-northeast-trend of the large extensional iron-carbonate zones is subparallel to the interpreted northeast-southwest sigma-1 axis of the D_2 deformation phase (Sanborn et al., 2001; Dubé et al., 2002). The northeast-southwest D_2 shortening may be responsible for the formation of these large extensional iron-carbonate zones of colloform-crustiform veins and breccia, although the possibility that they predate D_2 cannot be ruled out.

As elsewhere within the Red Lake mine trend, the iron-carbonate veins and breccia studied are barren to low grade (≤1–3 g/t Au). The spectacular colloform-crustiform banding in one large cockade breccia suggests that the CO_2-rich hydrothermal system was potentially formed at a higher crustal level, possibly 2 to 5 km from surface, than typical Archean quartz-carbonate shear-hosted ('mesothermal') gold deposits and thus shares some characteristics, especially in terms of vein textures, with high-level orogenic systems at Wiluna, Australia (Hagemann et al., 1994).

The high-grade gold mineralization is contained within an arsenopyrite-bearing silicified replacement zone. Evidence of silicified ('bleached') zones should be an important hydrothermal exploration target. As at the Campbell-Red Lake deposit, gold mineralization at Cochenour is also related to brecciation, silicification, and sulphidization (arsenopyrite) of the extensional colloform-crustiform iron-carbonate veins and breccia. However, on the Cochenour stripped outcrop, the intensity of brecciation, silicification, and sulphidization can be difficult to appreciate megascopically. Consequently, the gold content of these iron-carbonate veins and breccia should not be underestimated on the basis of the absence of visible brecciation, silicification, and arsenopyrite, as illustrated by sample KC-02-31 (Table 1). Silicification with associated arsenopyrite is clearly not as intense as in the Campbell-Red Lake deposit. The syn-D_2 timing of carbonate vein brecciation and silicification at the Red Lake mine is the critical element controlling high-grade gold deposition (Dubé et al., 2001a, 2002). On the outcrop studied, this relationship relative to D_2 is unclear, although iron-carbonate veins and gold mineralization predate the lamprophyre dykes and the black line faults. Gold mineralization at Cochenour has been interpreted as post-carbonate veining and late D_2 deformation (Sanborn, 1987).

In terms of exploration within the Red Lake mine trend, both the Cochenour and Red Lake mines are located on the limb of an F_1 fold refolded by F_2 folds, as recognized by Hutton (1965), with associated syn-D_2 axial planar higher strain zones (*see* Dubé et al., 2002). Such a structural position has potentially maximized the dilatation and hydrothermal fluid access and circulation in the F_2 hinge area.

The colloform-crustiform iron-carbonate veins and cockade breccia associated with gold mineralization are characteristic of the Red Lake district. The timing and genesis of these veins remain controversial, as originally recognized by MacGeehan and Hodgson (1982). In the study area, the presence of a locally carbonatized and foliated vesicular dyke cutting an iron-carbonate breccia vein (Fig. 2) indicates that iron-carbonate veins and breccia that accommodated a significant part of the D_2 strain are either early or pre-D_2. However, evidence of intense carbonatization locally developed in a lamprophyre dyke suggests that iron-carbonate hydrothermalism was active over a long period of time or that several stages of carbonatization occurred. New evidence from the Red Lake mine supports such a protracted multistage event with pre-, early and late to post-D_2 iron carbonate veining. First, a colloform-cockade iron-carbonate breccia vein cuts pyrrhotite-rich, ESC-style mineralization on level 23, suggesting that some carbonate veining is late to post-ESC-style mineralization (Fig. 5a; e.g. Dubé et al., 2002). Second, an exploration drift on level 16 reveals a section through the Huston conglomerate with some quartz-rich arenite and the faulted (activated) unconformity between the conglomerate and Balmer basalt (Fig. 5b, c). SHRIMP U-Pb dating elsewhere in the camp indicates that the Huston conglomerate is younger than 2.743 Ga (T. Skulski, pers. comm., 2002) and marks a regional unconformity between the 2.89 Ga Bruce Channel and the 2.75 to 2.73 Ga Confederation assemblages (e.g. Sanborn-Barrie et al., 2001). This conglomerate locally displays evidence for post-depositional iron-carbonate alteration. On level 16, the conglomerate is a polymictic proximal conglomerate or breccia (debris flow) dominated by subangular to subrounded laminated cherty clasts with local jasper-rich and green mica fragments; it is similar to the Timiskaming conglomerate (Fig. 5b, c, d). It is associated

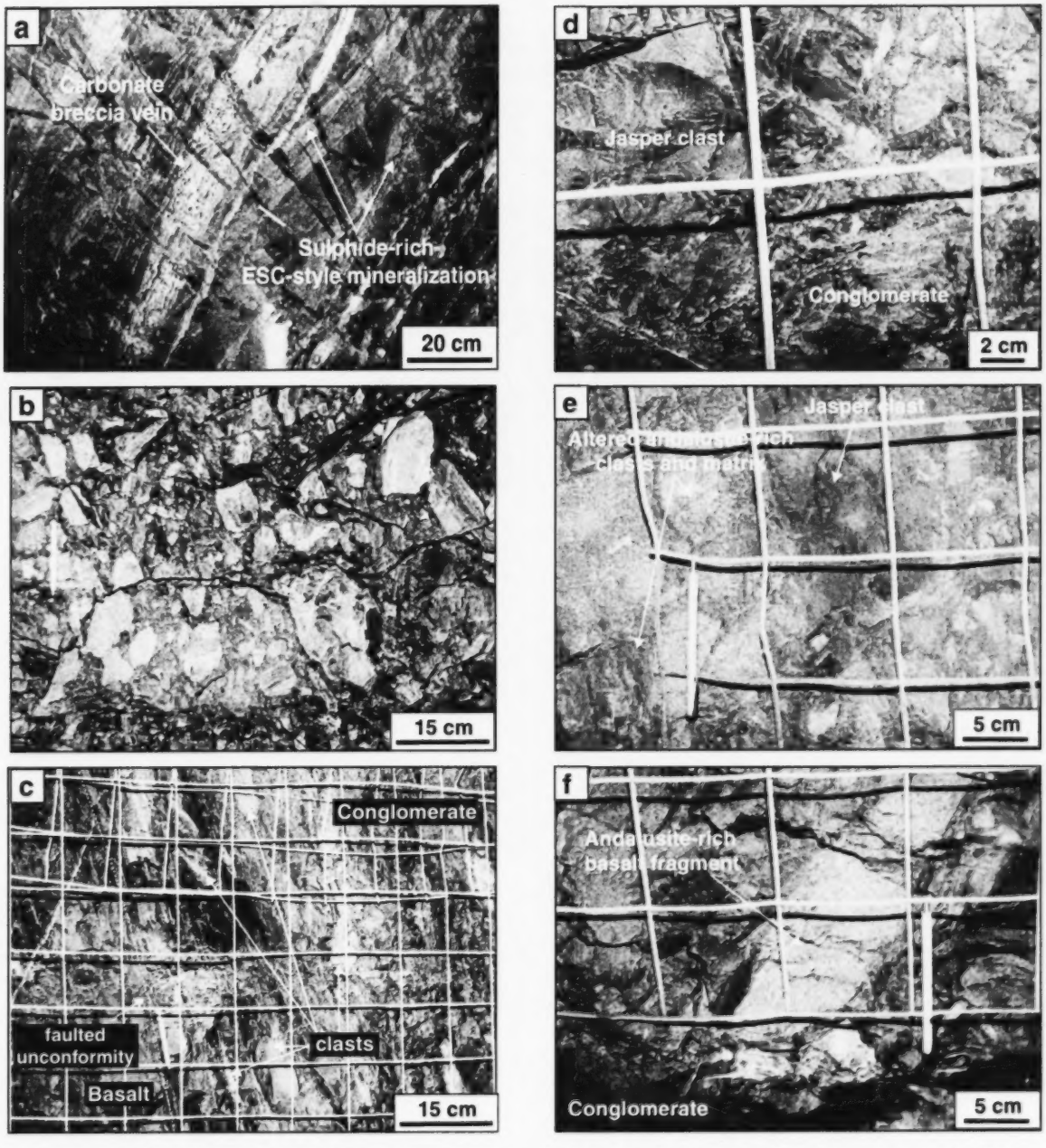

Figure 5. *a) ESC-style pyrrhotite-rich mineralization cut by cockade iron-carbonate barren breccia, section view, level 23; b) proximal polymictic Huston conglomerate (debris flow); c) section view showing the faulted (strained) unconformity between the foliated (S_2) Balmer basalt and the Huston conglomerate with flattened clasts; d) jasper-rich clast in Huston conglomerate; e) altered (sericite-quartz-andalusite) Huston conglomerate with preserved jasper clast; f) andalusite-rich clast of variolitic basalt in Huston conglomerate.*

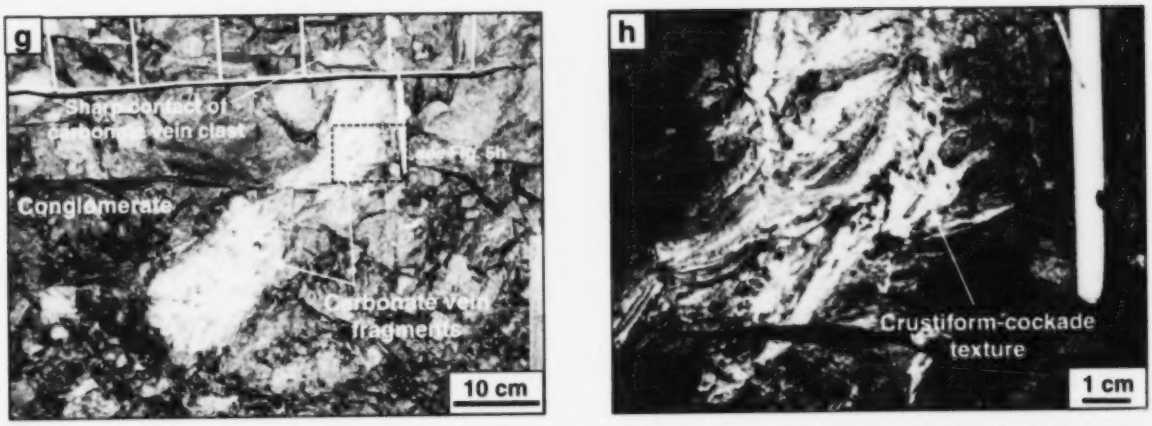

Figure 5. *g) two carbonate-vein clasts within Huston conglomerate; **h)** close-up of (g) showing crustiform-cockade texture in a carbonate clast.*

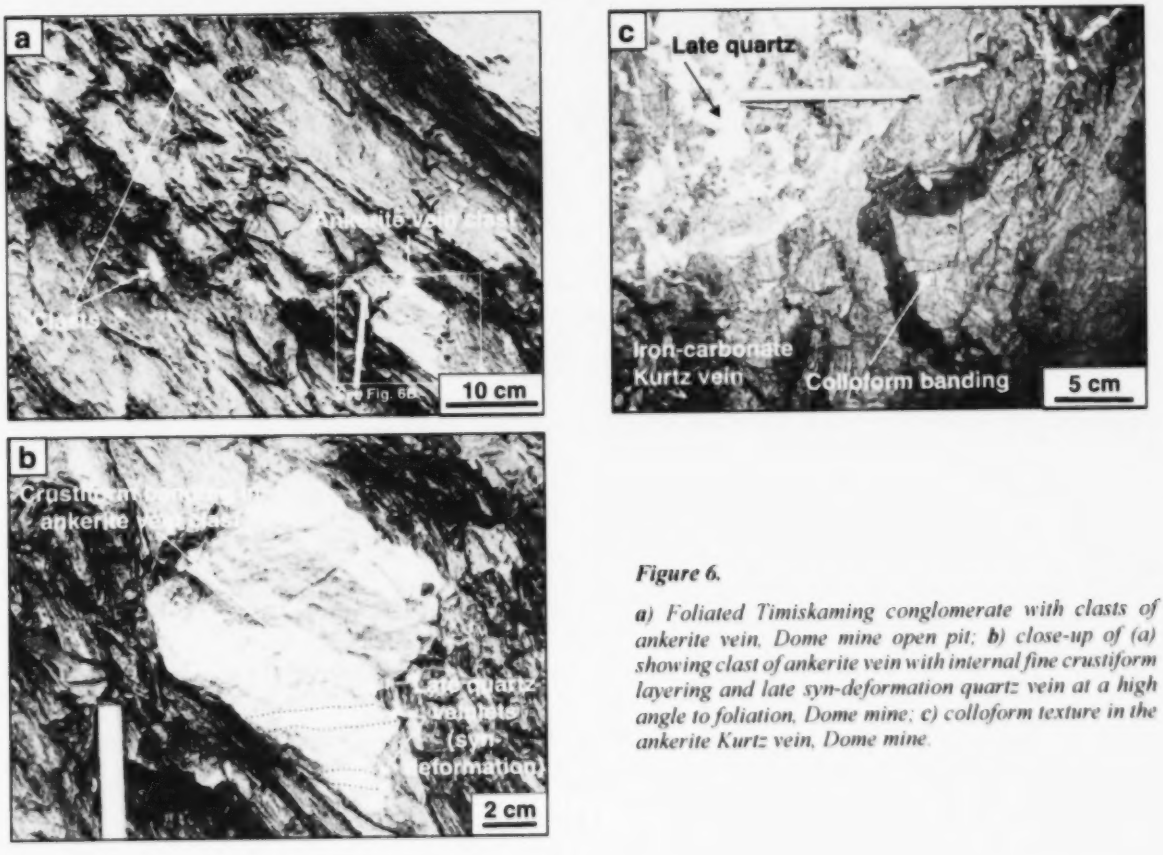

Figure 6.

a) *Foliated Timiskaming conglomerate with clasts of ankerite vein, Dome mine open pit; **b)** close-up of (a) showing clast of ankerite vein with internal fine crustiform layering and late syn-deformation quartz vein at a high angle to foliation, Dome mine; **c)** colloform texture in the ankerite Kurtz vein, Dome mine.*

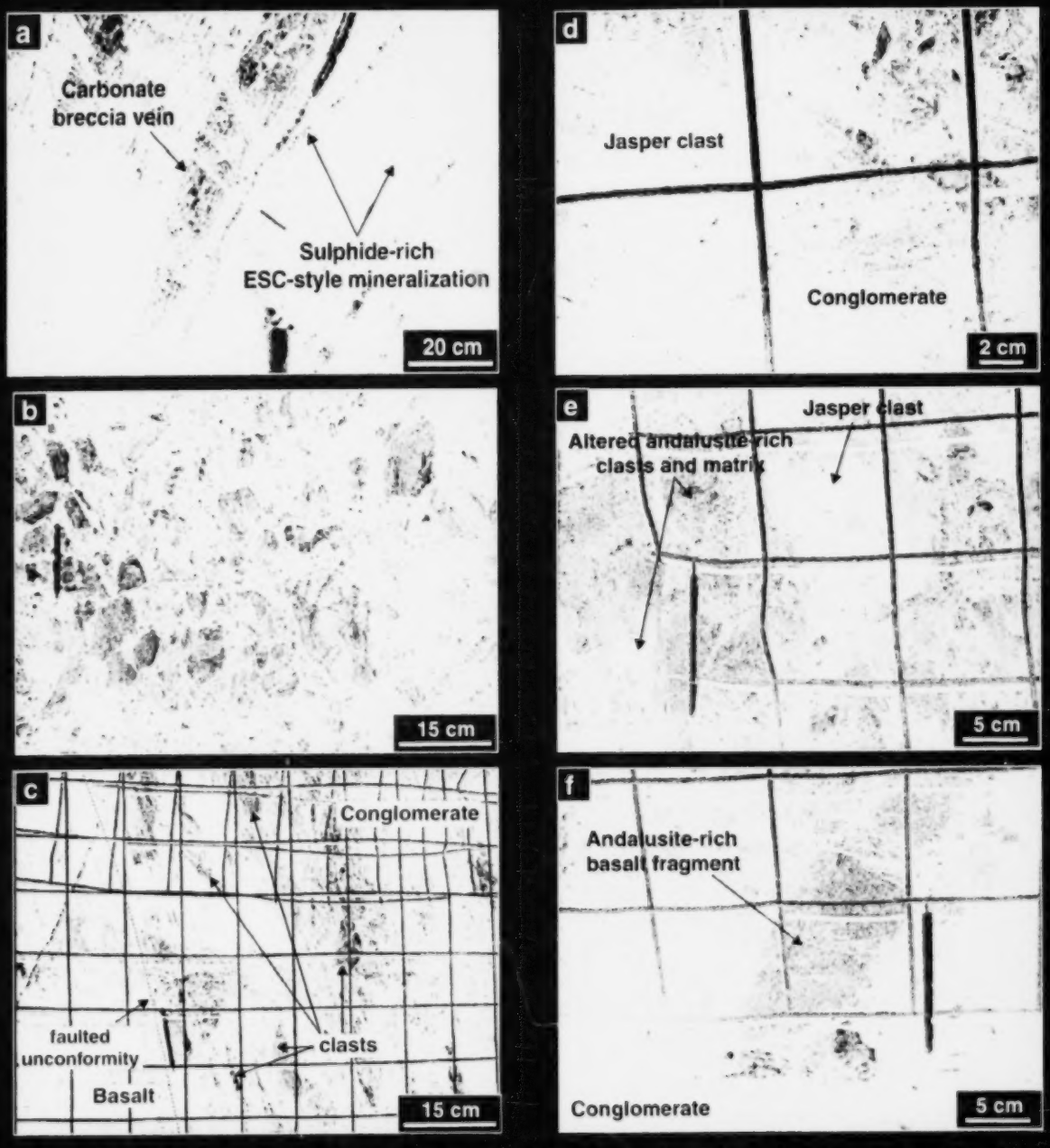

Figure 5. a) ESC-style pyrrhotite-rich mineralization cut by cockade iron-carbonate barren breccia, section view, level 23; b) proximal polymictic Huston conglomerate (debris flow); c) section view showing the faulted (strained) unconformity between the foliated (S_2) Balmer basalt and the Huston conglomerate with flattened clasts; d) jasper-rich clast in Huston conglomerate; e) altered (sericite-quartz-andalusite) Huston conglomerate with preserved jasper clast. f) andalusite-rich clast of variolitic basalt in Huston conglomerate.

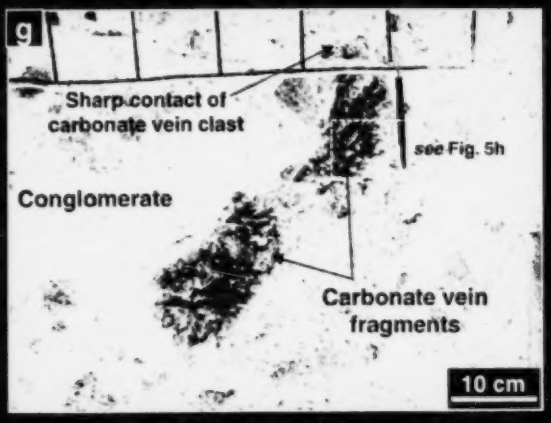

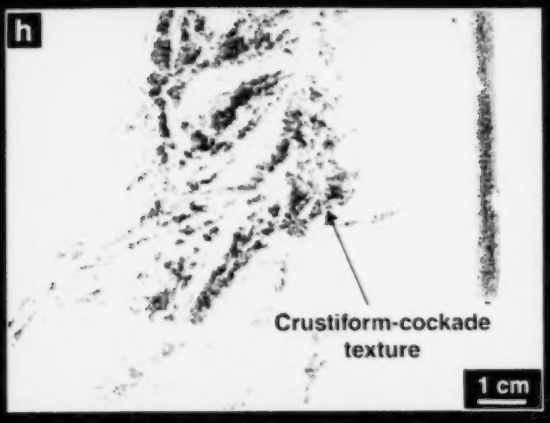

Figure 5. g) two carbonate-vein clasts within Huston conglomerate; h) close-up of (g) showing crustiform-cockade texture in a carbonate clast.

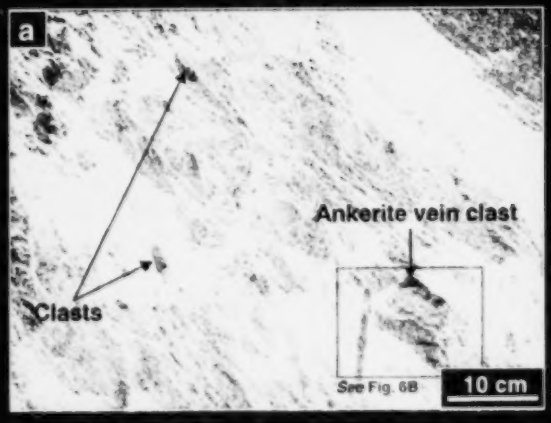

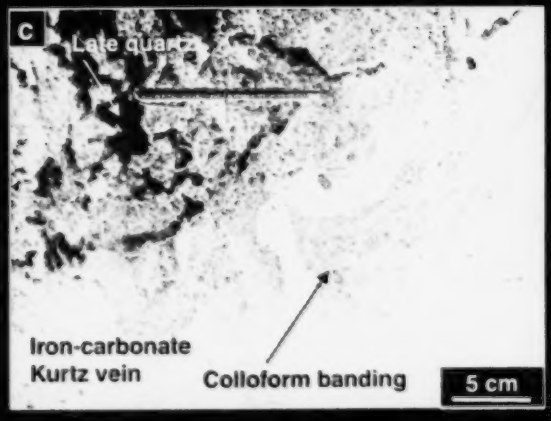

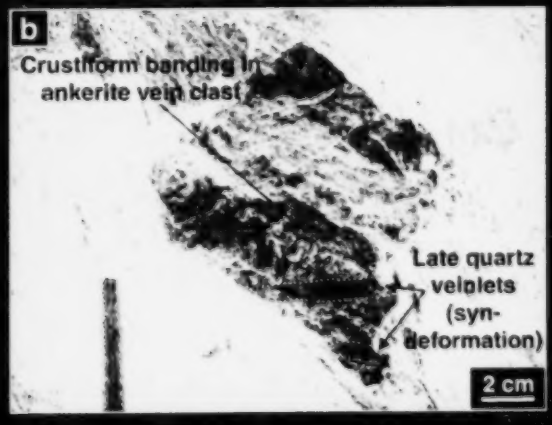

Figure 6.

a) Foliated Timiskaming conglomerate with clasts of ankerite vein, Dome mine open pit. b) close-up of (a) showing clast of ankerite vein with internal fine crustiform layering and late syn-deformation quartz vein at a high angle to foliation, Dome mine; c) colloform texture in the ankerite Kurtz vein, Dome mine.

with an exhumation probably caused by significant uplift and associated debris flow (possibly fault-scarp related), possibly in response to D_1 deformation (Sanborn-Barrie et al., 2001); it is contemporaneous with and possibly related to the 2.74 Ga onset of extensive magmatism and 6.4 km uplift proposed for the area by Stone (2000). On level 16, it is deformed by D_2. It is folded by F_2, clasts are locally flattened, and the matrix is foliated by S_2 (Fig. 5c). It is also locally strongly altered, as indicated by abundant sericite, quartz, and andalusite in both the matrix and the clasts (Fig. 5e). More importantly, it also contains clasts of andalusite-rich altered basalt (Fig. 5f) and a few local clasts of layered (possibly sheeted) carbonate veins with small crustiform banding and cockade texture that indicate pre- and syn-conglomerate aluminous alteration and pre-conglomerate iron-carbonate veining respectively (Fig. 5g, h). It is important to note that the aluminous alteration is spatially associated with gold mineralization at the Campbell-Red Lake deposit, forming an outer metre-wide alteration zone (Penczak and Mason, 1997; Dubé et al., 2002). Similar relationships with respect to carbonate veining were recently found at the Dome mine, where angular clasts of the famous laminated ankerite veins were found in the Timiskaming conglomerate (R. Keele and E. Barr, unpub. rept., 2002; Fig. 6a, b). The Campbell-Red Lake and Dome deposits share similarities (Dubé et al., 2002), in particular the presence of barren to low grade (≤1–4 g/t Au) colloform-crustiform iron-carbonate veins (Fig. 6c) beneath a folded regional unconformity and sedimentary trough; both display new evidence for pre-conglomerate (pre-regional unconformity) carbonatization. This new evidence along with data from Dubé et al. (2002) clearly indicate one or more protracted multistage alteration and veining events in the Red Lake mine trend with pre- and early-D_2 iron-carbonate and aluminous alteration followed by silicic replacement and gold as well as some late carbonatization and gold remobilization. This may help to understand the conflicting chronological relationships between aluminous alteration, carbonatization, mineralization, and deformation in the Red Lake mine trend. The position of the iron-carbonate veins beneath the subaerial unconformity may also help to understand their epithermal (near-surface) style. The analogy with the Dome mine suggests that the potential exists for significant east-southeast-trending mineralization within the Huston conglomerate and overlying Confederation assemblage in the F_2 fold hinge above the unconformity.

In terms of regional implications, the Cochenour deposit is located close to the Bruce Channel Formation and under a regional unconformity (Fig. 1). Such a spatial relationship with a regional unconformity also occurs the Campbell-Red Lake deposit, where the known mineralization is beneath the pre-D_2 Timiskaming-like Huston conglomerate; at the Madsen mine, the Austin tuff ore zones occur within or adjacent to the unconformity between Balmer and Confederation assemblages (Dubé et al., 2000; Sanborn-Barrie et al., 2000). This distribution clearly indicates that the presence of a regional unconformity between the Mesoarchean (3–2.89 Ga; Balmer, Ball, and Bruce Channel) and the Neoarchean Confederation assemblages (2.75–2.73 Ga) constitutes a first-order empirical exploration target as 25.9 M oz (94%) of the 27.6 M oz of gold found so far in the district (production, reserves, and resources) are contained in these three deposits adjacent to such an unconformity. Such an empirical relationship between significant gold deposits and an unconformity is also well known in Timmins, where the Timiskaming conglomerate either hosts or directly overlies the ore (Pamour and Dome mines), and also in Kirkland Lake, where the bulk of the ore is hosted by syenite porphyry intruding the Timiskaming conglomerate (e.g. Hodgson, 1993). Most gold mineralization in the Red Lake, Timmins, and Kirkland Lake districts postdates Timiskaming or Timiskaming-like unconformities, although these regional unconformities result from, or are associated with, one or more large-scale protracted tectonic (faulting and uplift), magmatic, and hydrothermal events to which large gold deposits are empirically spatially and possibly genetically related (e.g. Hodgson, 1993).

ACKNOWLEDGMENTS

Goldcorp Inc., particularly Gilles Filion, Stephen McGibbon, Tim Twomey, Rob Penczak, John Kovala, Matt Ball, Mark Epp, Michael Dehn, Kimberley DaPatro, and the entire production staff at the mine are thanked for their scientific contribution, logistic and financial support, critical review, and permission to publish. Matt Ball (Goldcorp Inc.) is thanked for showing KW the clasts of carbonate veins in the conglomerate at the Red Lake mine. Mary Sanborn-Barrie, Tom Skulski, and Jack Parker are thanked for constructive discussions in the field. Placer Dome is sincerely thanked for underground and open-pit visits at the Campbell and Dome mines and for sharing their knowledge. B. Dubé would like to sincerely thank M. Shannon, A. Verville, E. Barr, and D. Crimeen for providing a tour of the Kurtz vein and open pit at Dome, sharing their knowledge, and showing the ankerite vein clasts in the conglomerate. K. Williamson would like to acknowledge INRS for a scholarship. Critical review by Alain Tremblay improved the manuscript. We acknowledge NSERC, which provided a grant through a Parternership Agreement with NRCan's Earth Sciences Sector and Goldcorp Mine.

REFERENCES

Andrews, A.J., Hugon, H., Durocher, M., Corfu, F., and Lavigne, M.
1986: The anatomy of a gold-bearing greenstone belt: Red Lake, northwestern Ontario; Gold '86 Symposium, Toronto, p. 3–22.

Chi, G., Dubé, B., and Williamson, K.
2002: Preliminary fluid-inclusion microthermic study of fluid evolution and temperature-pressure conditions in the Goldcorp High-Grade zone, Red Lake mine, Ontario; Geological Survey of Canada, Current Research 2002-C27, 12 p.

Dubé, B., Balmer, W., Sanborn-Barrie, M., Skulski, T., and Parker, J.
2000: A preliminary report on amphibolite-facies, disseminated-replacement-style mineralization at the Madsen gold mine, Red Lake, Ontario; Geological Survey of Canada, Current Research 2000-C17.

Dubé, B., Williamson, K., and Malo, M.
2001a: Preliminary report on the geology and controlling parameters of the Goldcorp Inc. High Grade zone, Red Lake mine, Ontario; Geological Survey of Canada, Current Research 2001-C18.
2000-C17.

Dubé, B., Williamson, K., and Malo, M. (cont.)
2001b: The Goldcorp High-Grade Zone, Red Lake mine, Ontario: a photographic atlas of the main geological features; Geological Survey of Canada, Open File 3890.
2002: Geology of the Goldcorp Inc. High Grade zone, Red Lake mine, Ontario: an update; Geological Survey of Canada, Current Research 2001-C26.

Ferguson, S.A.
1966: Geology of Dome Township, District of Kenora, Ontario; Ontario Department of Mines, Geological Report 45, 98 p.

Giancola, D.
1994: Canadian Mines Handbook 1994–1995; Southam Magazine Group, 567 p.
1999: Canadian Mines Handbook 1999–2000; Southam Magazine Group, 624 p.

Hagemann, S.G., Gebre-Mariam, M., and Groves, D.
1994: Surface-water influx in shallow-level Archean lode-gold deposits in Western Australia; Geology, v. 22, p. 1067–1070.

Hodgson, C.J.
1993: Mesothermal lode-gold deposits. Mineral deposit modelling; Geological Association of Canada, Special Paper 40, p. 635–678.

Hopson, R.N.
1994: Alteration and mineralization in the '04' ore zone, Cochenour-Willians mine, Red Lake, Ontario; M.Sc. thesis, University of Western Ontario, London, Ontario, 230 p.

Horwood, H.C.
1945: Geology and mineral deposits of the Red Lake area, Ontario Department of Mines, Annual Report, v. 49, 231 p.

Hutton, D.A.
1965: Geology of the Cochenour Willans, Annco, and Wilmar gold-silver deposits, Red Lake, Ontario; Ontario Department of Mines, Open File Report 5078.

MacGeehan, P. and Hodgson, C.J.
1982: Environments of gold mineralization in the Campbell Red Lake and Dickenson mines, Red Lake district, Ontario; *in* Geology of Canadian Gold Deposits; Canadian Institute of Mining and Metallurgy, Special Volume 24, p. 184–207.

Nowlan, J.P.
1947: The geology of the Cochenour Willans gold mine, Red Lake, Ontario; The Precambrian, v. 20, p. 6–10.
1948: Cochenour-Willans mine; *in* Structural Geology of Canadian Gold Deposits; Canadian Institute of Mining and Metallurgy, Special Volume 1, p. 357–365.

Parker, J.R.
2000: Gold mineralization and wall rock alteration in the Red Lake greenstone belt: a regional perspective; *in* Summary of Field Work and Other Activities; Ontario Geological Survey, Open File Report 6032, p. 22-1–22-28.

Penczak, R. and Mason, R.
1997: Metamorphosed Archean epithermal Au-As-Sb-Zn-(Hg) vein mineralization at the Campbell Mine, northwestern Ontario; Economic Geology, v. 92, p. 696–719.

Pirie, J.
1982: Regional geology and setting of gold deposits, eastern Red Lake area, northwestern Ontario; Canadian Institute of Mining and Metallurgy, Special Volume 24, p. 171–183.

Sanborn, M.
1987: The role of brittle-ductile shear in the formation of gold-bearing quartz-carbonate veins in the West Carbonate Zone of the Cochenour Willans gold mine, Red Lake, Ontario; M.Sc. thesis, University of Toronto, Toronto, Ontario, 148 p.

Sanborn-Barrie, M., Skulski, T., Parker, J., and Dubé, B.
2000: Integrated regional analysis of the Red Lake belt and its mineral deposits, western Superior Province, Ontario; Geological Survey of Canada, Current Research 2000-C18.

Sanborn-Barrie, M., Skulski, T., and Parker, J.
2001: Three hundred million years of tectonic history recorded by the Red Lake greenstone belt, Ontario; Geological Survey of Canada, Current Research 2001-C19.

Stone, D.
2000: Temperature and pressure variations in suites of Archean felsic plutonic rocks, Berens River area, northwestern Superior Province, Ontario, Canada; Canadian Mineralogist, v. 38, p. 455–470.

Geological Survey of Canada Project PS 2011